# Functionalization of Porous Carbon Materials with Designed Pore Architecture

By *Andreas Stein,* Zhiyong Wang,* and *Melissa A. Fierke*

**Recent progress in syntheses of porous carbons with designed pore architecture has rejuvenated the field of carbon chemistry and promises to provide new advanced materials. In order to reap the full benefit of designer carbons, it is necessary to develop chemistries for functionalizing the porous carbon surfaces. This Review examines methods of functionalizing porous carbon through direct incorporation of heteroatoms in the carbon synthesis, surface oxidation and activation, halogenation, sulfonation, grafting, attachment of nanoparticles and surface coating with polymers. Methods of characterizing the functionalized carbon materials and applications that benefit from functionalized nanoporous carbons with designed architecture are also highlighted.**

## 1. Introduction

Over the last two decades, tremendous progress has been made in controlling the structure of porous materials, over length scales ranging from molecular to bulk dimensions. Templating methods with surfactants and polymers, for example, have spawned research efforts across the globe, leading to thousands of publications that describe mesostructured, mesoporous, macroporous, and hierarchically structured porous materials (Fig. 1). Initially, the focus was largely on silica-based systems and some other oxides. While these systems continue to be very important, increasing attention has been paid to porous carbon materials with designed pore architecture over the past few years, and annual publications on this topic are on the rise. Some researchers consider nanoporous carbons as "the next generation of mesoporous materials."[1] Porous carbon is attractive because it can be prepared relatively inexpensively from a wide variety of low-cost precursors, it is typically biocompatible and quite chemically stable under nonoxidizing conditions, it has low density, high thermal conductivity, good electrical conductivity, mechanical stability and is easily handled. As a high specific surface-area material, porous carbon can be used as an effective sorbent, catalyst support, filter, and electrode for a range of applications, some of which will be discussed later. Compared to mesoporous silica, mesoporous carbon is more resistant to structural changes by hydrolytic effects in aqueous environments.

Although the concept of structuring porous carbon by templating was already demonstrated in 1982,[2] it was more widely adopted when ordered mesoporous silica became readily available as a mold. Ryoo et al. showed that the mesopores could be filled with a carbon precursor, such as sucrose, which could then be processed to form a carbon replica structure (a structural "negative") of the silica mold.[3] Elimination of silica by extraction resulted in a mesoporous carbon product, whose architecture was dictated by the silica preform. Since then, many other carbon precursors besides sucrose[3–7] have been utilized, including furfuryl alcohol,[5,8–10] ethylene,[11] propylene,[12] phenol-formaldehyde[12–16] and resorcinol-formaldehyde resins,[17–21] acetonitrile,[22] polypyrrole,[23] mesophase and petroleum pitches,[24–26] and other aromatic precursors,[27,28] such as naphthalene, anthracene, pyrene, benzene, styrene, and acenaphthene. With suitable molds, it is possible to control both the internal morphology (ordered or disordered micro-, meso-, and

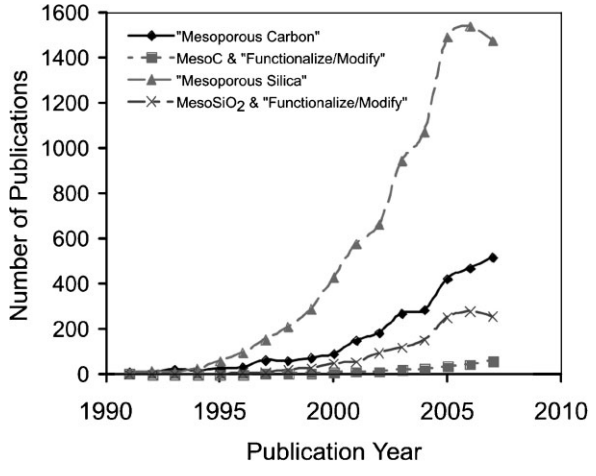


**Figure 1.** Trends in the number of publications listed by SciFinder Scholar (trademark of the American Chemical Society) on May 9, 2008, for the following search terms: "mesoporous carbon"; "mesoporous carbon" and "functionalize" or "modify"; "mesoporous silica"; "mesoporous silica" and "functionalize" or "modify". The numbers for mesoporous carbon continue to rise annually.

[*] Prof. A. Stein, Z. Wang, M. A. Fierke
Department of Chemistry, University of Minnesota
207 Pleasant St. S.E., Minneapolis, MN 55455 (USA)
E-mail: a-stein@umn.edu

**DOI: 10.1002/adma.200801492**



© 2008 WILEY-VCH Verlag GmbH & Co. KGaA, Weinheim

macropores) and the external morphology of the porous carbon products (powders, films and membranes, spheres, rods, cubes, tetrapods, fibers, nanowires and monoliths).[10,21,25,29–35] Besides ordered mesoporous silica and aluminosilica,[36,37] colloidal particles[38–43] and colloidal crystals[12,21] can also serve as hard templates for porous designer carbons. More recently, nanocasting methods have been supplemented by direct soft-templating methods that eliminate the need for a silica preform. The latter methods involve direct syntheses using self-assembled supramolecular aggragates of surfactants or block-copolymers as templates and in some cases copolymerization of carbon precursors with metal alkoxides.[14,18,44–57] By combining multiple hard- and soft-templating methods, hierarchical carbon structures with designed porosity on multiple length scales can be obtained.[6,10,34,35,58–63] Methods of preparing carbon materials with ordered porosity have been reviewed by several authors.[29,36,37,64–67]

Just as mesoporous silica became more versatile after procedures had been developed to functionalize the silica surfaces or framework,[68] porous carbons can be elevated to the next level of utility by surface functionalization to fine-tune interactions with guest molecules and to optimize the bulk and interfacial properties of the materials. Methods to modify surfaces of porous designer carbons are just starting to be

Andreas Stein earned his Ph.D. degree with Prof. G.A. Ozin at the University of Toronto. In 1994 he joined the faculty at the University of Minnesota, where he is now a Distinguished McKnight University Professor of Chemistry. Professor Stein's research interests are in the field of solid-state chemistry, in particular porous materials and nanocomposites. His program has pioneered research on the compositional and structural control of templated mesoporous/macroporous sieves, nanoparticle shaping, open-framework structures, and polymer/inorganic nanocomposites.


Zhiyong Wang was born in Handan, Hebei Province, China. He obtained a B.S. degree at the University of Science and Technology, Hefei, Anhui Province, in 2003. He is currently pursuing his Ph.D. degree under the supervision of Prof. A. Stein.

Melissa Fierke was born in Owatonna, Minnesota, U.S.A. She obtained a B.A. degree in chemistry at Concordia College, Moorhead, Minnesota. She is currently pursuing her Ph.D. degree under the supervision of Prof. A. Stein.


WILEY InterScience® DISCOVER SOMETHING GREAT

© 2008 WILEY-VCH Verlag GmbH & Co. KGaA, Weinheim

developed.[29,66] Fortunately, researchers can build on the significant base of knowledge associated with functionalization of more traditional forms of carbon (activated carbon, coal, glassy carbon electrodes) and also on recent methods of functionalizing carbon nanotubes.[69–72] Although this precedence is very useful, the new porous carbon systems sometimes create unique challenges, which are related to issues of confinement, diffusion, strongly curved surfaces, and – in electrochemical reactions – potentially high electric fields in the small pores. Certainly, methods of functionalizing porous carbons have not yet matured to the level of porous silica, but they are rapidly gaining momentum. Characterization of the modified carbon samples brings additional challenges that are also being addressed in current research.

Here, we will review methods of modifying surfaces of templated nanoporous carbons (TNCs) with charged and neutral molecular surface groups, polymers, and nanoparticles. When we use terms like TNC, ''designer carbon'', or ''synthetic porous carbon'' in this review, we mean to include only synthetic carbons, whose porosity is controlled during the synthesis, typically by a template. When the discussion concerns more traditional mesoporous or microporous carbons (e.g., carbon black or activated carbon), this is stated explicitly. However, because at this stage the number of papers describing surface functionalization of designed porous carbons is relatively small, we will also draw on some examples of methods to modifying other forms of carbon when they are likely to be applicable to synthetic porous carbons. We are using a relatively generous definition of ''functionalization'', and will include, for example, composite structures in which a porous carbon entraps nanoparticles or biological molecules, even without covalent bond formation. Sample characterization methods will be briefly outlined, and the benefits of surface modification for specific applications (sensors, batteries, fuel cells, capacitors, hydrogen storage, catalysis, sorption, and magnetic materials) will be described.

## 2. Functionalization

### 2.1. Direct Synthesis

An efficient way of incorporating functionality (covalently attached heteroatoms or highly dispersed nanoparticles) in porous carbon materials is directly during their synthesis. This is possible by two different approaches: nanocasting with heteroaromatic precursors, using solution or chemical vapor-phase infiltration, or direct multiconstituent-coassembly methods, which do not require a separate mold. Similar to observations in hybrid mesoporous silicates, these approaches ensure more uniform distributions of functional groups in the mesoporous products and avoid pore blocking, which is sometimes associated with post-synthesis grafting.

Syntheses of hybrid organic–inorganic silicate structures rely largely on the availability of organosiloxanes with ≡Si–C–R bonds and different –R groups. For the direct syntheses of porous carbon materials, the variety of possible organic precursors containing heteroatoms is in principle very large, limited mainly by their propensity to form polymers that can be carbonized and by their resistance to decomposition during the carbonization process. Suitable precursors include nonaromatic compounds, such as acrylonitrile,[73] and heteroaromatic compounds, such as thiophene, furan and pyrrole, for S, O, and N groups, respectively.[74]

Several studies demonstrated direct syntheses of N-doped mesoporous carbon samples that are based on nitrogen-containing precursor molecules. So far, this work has relied largely on nanocasting techniques. The first reported mesoporous carbon material with nitrogen functionality was prepared by solution-phase infiltration of the mesoporous silica SBA-15, with an acrylonitrile solution containing the initiator 2,2′-azobisisobutyronitrile.[73] Following radical polymerization to produce a polyacrylonitrile (PAN) homopolymer, the polymer was stabilized by low-temperature thermal treatment in air, and then was carbonized. The silica template was removed by etching with HF solution, to produce ordered mesoporous carbon samples with either monomodal or bimodal pore size. In the bimodal pore systems, one set of pores resulted from replicating the silica template walls. The other set of pores was ascribed to partial removal of PAN-based carbon during the carbonization procedure. Depending on the stabilization temperature, the nitrogen content varied from 4 to 15 mol %. The specific identity of the nitrogen groups was not identified in this early report. An alternate nitrogen-doped carbon precursor, melamine-formaldehyde, was used for nanocasting mesoporous carbon spheres from fumed silica particles.[75] As a result of their large surface areas ($1460\,m^2\,g^{-1}$) and nitrogen groups (6 wt %), which enhanced wettability and conductivity of the carbon, the porous products exhibited high specific capacitance values, up to $159\,F\,g^{-1}$ at $0.5\,A\,g^{-1}$ and $130\,F\,g^{-1}$ at current densities of $20\,A\,g^{-1}$, making the materials interesting for supercapacitors. Aniline is yet another precursor for nitrogen-doped mesoporous carbon prepared by nanocasting.[76]

Specific N-containing groups, namely pyridine groups, were introduced by cyclotrimerization of diethynylpyridines with various substitution patterns within mesoporous silica, acting as a hard template.[77] Depending on the substitution, the diethynylpyridine precursors could be prealigned on the silica surface through hydrogen bonding interactions between nitrogen atoms and silanol groups. The mesostructural order and pore texture were affected by the substitution patterns. In these samples, some nitrogen was lost during carbonization.

Mesoporous carbon nitride samples were nanocast by polymerizing and pyrolyzing a mixture of ethylenediamine and carbon tetrachloride within the pores of either mesoporous silicas SBA-15 or SBA-16.[78,79] By varying the ratio of carbon to nitrogen in the source, the degree of polymerization, and hence textural parameters, were controlled.[80]

Sulfur-functionalized mesoporous carbons were prepared by nanocasting using linear polymerization of 2-thiophenemethanol, i.e., Friedel–Crafts alkylation chemistry.[74] The mesoporous products contained 4–7 wt % sulfur, had high surface areas ($1400–1930\,m^2\,g^{-1}$), and large pore volumes, exceeding $2\,cm^3\,g^{-1}$. These materials showed excellent affinity for Hg under wide pH conditions, pH 1.0–12.8, i.e., including conditions when silica-based supports become unstable. The saturation binding capacity was higher and the Hg sorption kinetics faster than in sulfur-impregnated activated carbon.


© 2008 WILEY-VCH Verlag GmbH & Co. KGaA, Weinheim

Relatively high levels of surface oxygen groups can be produced by hydrothermal carbon syntheses. One example involves carbon nanocast from an ordered mesoporous silica template with an aqueous furfural solution as the carbon precursor. When carbonization is carried out hydrothermally, at a comparatively low temperature of 180 °C, the process yields ordered hydrothermal carbon with hydrophilic carbon surfaces.[81] These surfaces can be further functionalized by appropriate grafting methods (see below).

Another versatile method involves chemical vapor deposition (CVD), since it permits easy penetration of volatile precursors into the pores of a hard template, whether they be small micropores (zeolite templates) or larger mesopores (mesoporous silica templates). With acetonitrile as a CVD precursor, the N-doped carbon products have a highly graphitic nature.[11,22,82] The surface areas and pore volumes of graphitic, nitrogen-containing mesoporous carbons tend to be lower than for carbons with amorphous walls.[82] Whereas the mesostructural order decreases and the graphitic content increases with increasing CVD temperature, the typical nitrogen content (ca. 8–8.5 mol %) changes little with temperature in the range 850–1000 °C.[22] Nitrogen was assigned to highly coordinated (quaternary) and $sp^2$ pyridine-like forms.[82] This synthesis has been extended to produce monolithic products with reasonably high hydrogen-uptake capacity, up to 3.4 wt % at 20 bar and −196 °C.[83] Pyrrole is another suitable CVD precursor for N-doped mesoporous carbons, having a relatively high vapor pressure even at room temperature.[23] In this case, a mesoporous silica template is first impregnated with $FeCl_3$ as the oxidant for formation of polypyrrole. Because oxidative polymerization is stoichiometric between pyrrole and $FeCl_3$, the loading of polymer and, subsequently, carbon, is readily controlled. Typically attained nitrogen contents are around 5.5 mol %.[23]

As an alternative to nanocasting, the cooperative assembly between resols, block-copolymers, and perhaps additional components can produce ordered mesoporous carbons, in a process that obviates the use of a separate hard template.[45,47,51,84] Such cooperative assembly reactions have recently been extended to precursors that introduce heteroatoms into the carbon structures. For example, by adding *p*-fluorophenol to a phenol-formaldehyde mixture with a triblock copolymer as a structure-directing agent, covalent C–F bonds are introduced in the resulting mesostructured polymers, and are maintained after carbonization at 900 °C.[57] The functionalized phenol affects the mesostructure, which can be tuned through the *p*-fluorophenol/phenol ratio. In addition to their relatively high surface areas (up to 1000 $m^2 g^{-1}$) and narrow mesopore size distributions, the fluorinated mesoporous carbons exhibit higher electron-transfer rates than similar carbons lacking the fluorine groups.

A coassembly reaction is suitable not only for introduction of molecular functional groups to mesoporous carbons, but also allows dispersion of nanoparticles throughout the carbon walls. For example, mesoporous carbon composites containing highly dispersed titanium carbide nanoparticles were synthesized from the coassembly of the triblock copolymer Pluronic F127, a phenol-formaldehyde mixture, and titanium citrate, using a solvent-evaporation-induced self-assembly (EISA) approach to obtain 2D hexagonal mesostructures.[85] After thermal curing, the sample underwent in situ carbothermal reduction in Ar above 950 °C, producing a mesoporous product with cubic titanium carbide nanoparticles throughout the amorphous carbon framework. In this synthesis, the citrate ligand plays the important role of suppressing titania crystallization and macrophase separation at temperatures below which the rigid carbon framework forms. It therefore ensures that an ordered mesostructure is obtained in these composites. Furthermore, it stabilizes the titanium precursor in water, making the reaction less sensitive to relative humidity. With prehydrolyzed $TiCl_4$ as the titanium precursor, embedded anatase-type $TiO_2$ particles are obtained instead.[86] The resulting ordered mesoporous C-$TiO_2$ nanocomposites are catalytically active for the photodegradation of organic dyes that adsorb on the glassy carbon phase.

### 2.2. Surface Oxidation

When functional groups are not included directly during the synthesis of porous carbon materials, controlled oxidation may be used to introduce oxygen-containing groups (such as ketone, phenol, lactone, lactol, ether, carboxylic acid, and carboxylic anhydride groups, see Fig. 2) on the carbon surface, and prepare the sample for subsequent modification by covalent, electrostatic, and hydrogen-bonding interactions. Furthermore, careful oxidation enhances the wettability of the pores by polar solvents and increases the fraction of micropores and the surface area of the carbon. Oxygen-containing surface groups can also enhance the electrochemical capacitance of carbon materials.[88] The extent of oxidation depends on the strength of the oxidants, which include oxidizing gases (air, oxygen, ozone, nitrous oxide, nitric oxide) and oxidizing solutions (e.g., nitric acid, hydrogen peroxide, hypochlorite, persulfates, permanganates, dichromates, chlorates).[89–93] Oxidation conditions must be carefully chosen to prevent excessive corrosion and structural breakdown of the carbon skeleton. The use of a mild oxidant, such as hypochlorite, provides an opportunity for tuning the surface properties.[91] The type of oxidant also influences the composition of surface groups. For example, in comparison with ozone treatment, air oxidation produces more phenol and fewer lactone/anhydride groups.[93] It should be kept in mind that not all surface oxides are stable. Surface oxides can be irreversibly removed by reduction in KOH, using a cathodic potential sweep.[88] These unstable surface oxygen-containing groups could be desorbed from the carbon surface as $CO_2$ and CO, as monitored by temperature-programmed desorption. The removal of surface oxygen groups via heat treatment creates additional micropores.[92]

The most commonly used oxidant for carbonaceous materials is an aqueous solution of either concentrated or dilute nitric acid.[88,90–92] Oxidation with nitric acid is a highly efficient process for the generation of surface functional groups, and is quite controllable, simply by tuning the acid concentration, temperature, and treatment duration. For these reasons, this oxidation technique has also been applied successfully to the surface modification of ordered mesoporous carbons, resulting in carboxyl groups.[94–97] It is worth noting that the mechanical strength of an oxidized carbon sample is determined by the structure of the pristine mesoporous carbon. For some ordered mesoporous carbons, it was observed that the extent of structural


WILEY InterScience® DISCOVER SOMETHING GREAT

© 2008 WILEY-VCH Verlag GmbH & Co. KGaA, Weinheim

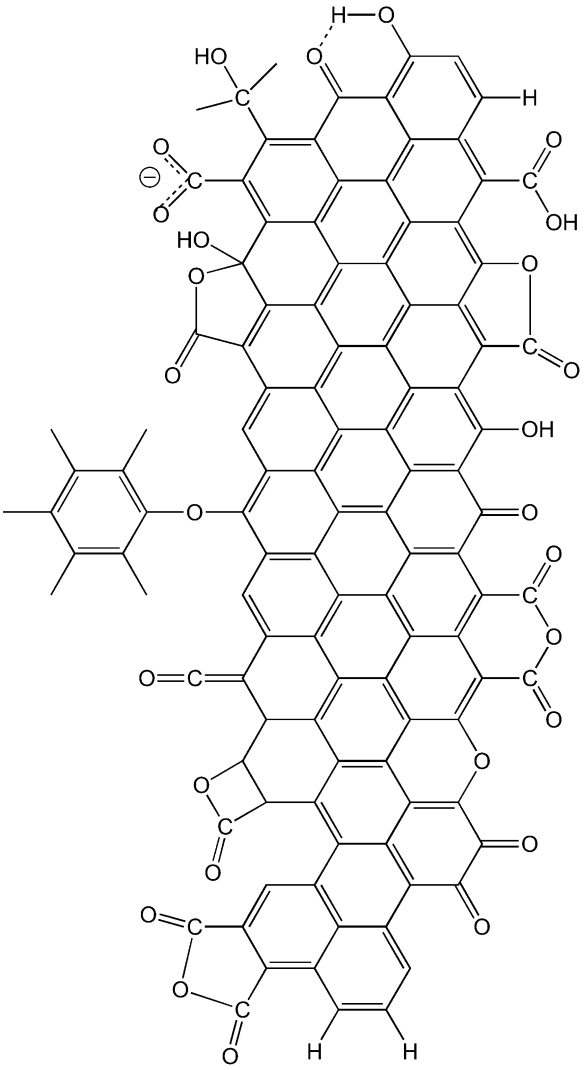

**Figure 2.** Schematic diagram summarizing possible surface groups on oxidized TNCs. Adapted from Fanning et al. [87].

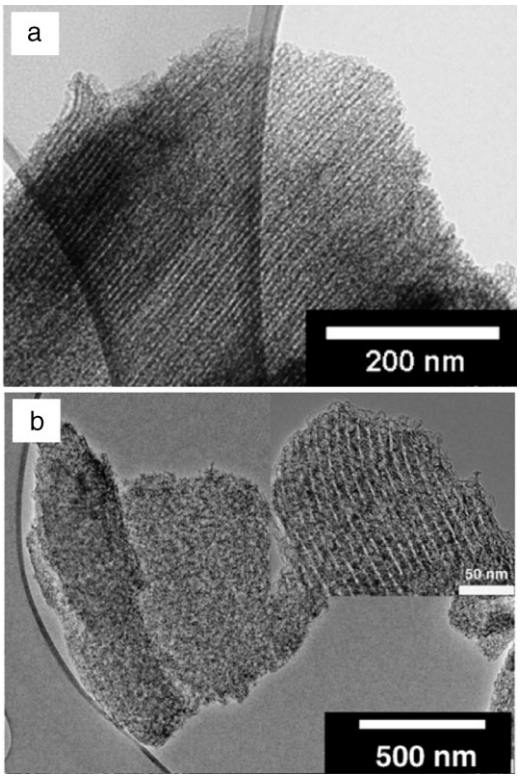


**Figure 3.** TEM images of ordered mesoporous carbon CMK-5 oxidized by nitric acid using different conditions: a) 1 M $HNO_3$ at 90 °C and b) 4 M $HNO_3$ at 130 °C. Reproduced with permission from Bazula et al. [94]. Copyright Elsevier 2008.

degradation after oxidation exceeded that of disordered carbons treated under the same conditions.[94,96] Even among ordered mesoporous carbons, oxidation can have different effects. For example, the ordered mesoporous carbon CMK-5 is prone to destruction during oxidation (Fig. 3), even when a mild oxidant such as hydrogen peroxide is used.[96] However, CMK-3 was found to be more robust than CMK-5 after oxidation.[94,97] This discrepancy could be explained by the difference in mesostructures. CMK-3 is prepared by volume templating from ordered mesoporous silica SBA-15, whereas CMK-5 is prepared by surface templating, using the same template. The structures of these materials can be described as piles of bundles of carbon rods (for CMK-3) or tubes (CMK-5) connected with carbon bridges. The bridges in CMK-3 are probably thicker and less reactive to an oxidant, which may contribute to the greater stability of CMK-3 during modification reactions.

Porosity changes after nitric acid oxidation are different for carbons with different pore sizes. For mesoporous carbons, the response to oxidation can be quite complex. In the case of an ordered mesoporous carbon, the Brunauer–Emmett–Teller (BET) surface area and the porosity first increased and then decreased after nitric acid treatment.[97] The initial increase was considered to be the result of micropore generation. However, longer oxidation caused partial structural collapse, which resulted in the observed drop in surface area and pore volume. On the other hand, both of these parameters increased for 3D ordered macroporous (3DOM) carbon after similar treatment.[98] This discrepancy in behavior may be explained by the difference in wall dimensions. The framework of 3DOM carbon is built with connections that are ca. 50 nm thick, making the 3DOM structure moderately more robust towards oxidation than mesoporous carbons, with wall thicknesses in the nanometer or subnanometer range. After controlled oxidation, the macroporous structure is retained even when the surface is etched to produce additional microporosity, which enlarges the BET surface area and total porosity.[98] However, even for 3DOM carbon monoliths, extended oxidation results in significant etching of the surface microstructure, and increases the brittleness of the monoliths. Oxidation also decreases the electronic conductivity of the porous carbons, which is unfavorable for applications that rely on porous carbon as an electrode.[34]

One aim of controlled surface oxidation is to produce anchoring points for additional surface groups and pore size manipulation, e.g., by an esterification reaction between carboxyl groups and alcohols.[94] Grafting procedures will be discussed in


© 2008 WILEY-VCH Verlag GmbH & Co. KGaA, Weinheim

more detail later on. Treatment of porous carbon with nitric acid can also be used to introduce surface charge onto the carbon surfaces. For example, after nitric acid oxidation of 3DOM carbon, carboxylic acid groups are transformed to negatively charged carboxylate groups by neutralization with dilute sodium hydroxide solution. The relatively small negative surface charge may be enhanced by deposition of multiple polyelectrolyte layers, facilitating attachment of charged nanoparticles through electrostatic interactions (see later).[98]

### 2.3. KOH Activation/$CO_2$ Activation

Alteration of the sample texture also occurs by activation of carbon with KOH or $CO_2$. For example, high-temperature treatment (750 °C) of a physical mixture of KOH with the ordered mesoporous carbon CMK-8 generated micropores by framework etching, as the carbon was oxidized to carbonate ions and related species.[99] This resulted in a significant increase in the BET surface area and micropore volume, but also in a decrease in mesostructural order and average mesopore diameters. The alkali metal that was introduced into the carbon could be removed by washing. Activation of mesoporous carbon with $CO_2$ at an elevated temperature (950 °C) led to similar changes in texture,[100] although at temperatures up to 700 °C the mesostructure of the mesoporous carbon FDU-15 was quite stable.[101] Similarly, when KOH activation was performed at 700 °C, mesoporosity was preserved in phenolic resin-based carbons, while microporosity was substantially increased.[102]

### 2.4. Sulfonation

Porous carbon materials functionalized with sulfonic acid groups have been investigated as potential, environment-friendly solid-acid catalysts. Functionalized carbons eliminate the need for liquid acids in certain catalytic reactions, and may be reused many times. Mesoporous carbon synthesized by carbonization of starch and polysaccharides was sulfonated by suspension in sulfuric acid at elevated temperature.[103] The product had a sulfonate concentration of 0.5 mmol $g^{-1}$, and provided high conversion, selectivity, and reaction rates for several catalytic reactions. Ordered mesoporous carbons were functionalized with sulfonic acid groups by reduction of a diazonium salt, 4-benzene-diazoniumsulfonate, by hydrophosphorous acid.[104] This method provided a coverage of 1.93 mmol $g^{-1}$ under relatively mild conditions, and the product was successfully used as a catalyst for esterification and condensation reactions. An ordered mesoporous carbon was also functionalized with sulfonate groups by contacting the carbon with the vapor of fuming sulfuric acid inside an autoclave.[105] Under optimal conditions, a surface concentration of 1.3 mmol $g^{-1}$ was achieved on this material, which served as an active and selective catalyst for several catalytic reactions, including rearrangement and condensation reactions.

### 2.5. Halogenation

Surface modification can drastically change the physical properties of carbon materials. Fluorination is used to create a hydrophobic carbon surface. Fluorine is introduced to the carbon surface by a variety of methods. Mesoporous carbons have been functionalized directly by flowing diluted $F_2$ gas over the sample for four days at different temperatures, ranging from room temperature to 250 °C.[106] Using this method, fluorine reacts with hydrogen atoms in C–H bonds, and also with unsaturated bonds of the carbon. Depending on the experimental conditions, F:C ratios can vary from 0.1 to 0.8. Mesoporous carbons have also been modified with fluoroalkylsilane. After the initial oxidation of the surface, the carbon is reacted with the hydrolyzed fluoroalkylsilane $(CF_3(CF_2)_7CH_2CH_2Si(OCH_3)_3$.[107] The functionalized carbon is superhydrophobic, exhibiting a very high water contact angle and low water adsorption (Fig. 4). Carbon foams have also been functionalized with fluorous compounds. A Teflon-like nanocoating was deposited onto foams from fluorocarbon monomers such as $CF_4$ and $C_3F_8$ in a microwave plasma reactor, making the composite material more inert to degradation by atmospheric moisture and pollutants.[108]

Surface bromination provides a starting point for subsequent conversion into other functional groups, such as amines, anilines, alcohols, or thiols. In the case of carbon blacks, halogenation with bromine (and also chlorine) is possible by high-temperature treatment with the halogen.[109] The reactions occur by substitution of hydrogen with evolution of hydrogen halide. These halogenation reactions should also be feasible for synthetic nanoporous carbons, given their relatively high hydrogen content and similar atomic structures.

### 2.6. Grafting

Probably the largest variety of surface functional groups on porous carbons is accessible by grafting techniques (Fig. 5). In some of these methods, the carbon surface has a preexisting surface functionality,

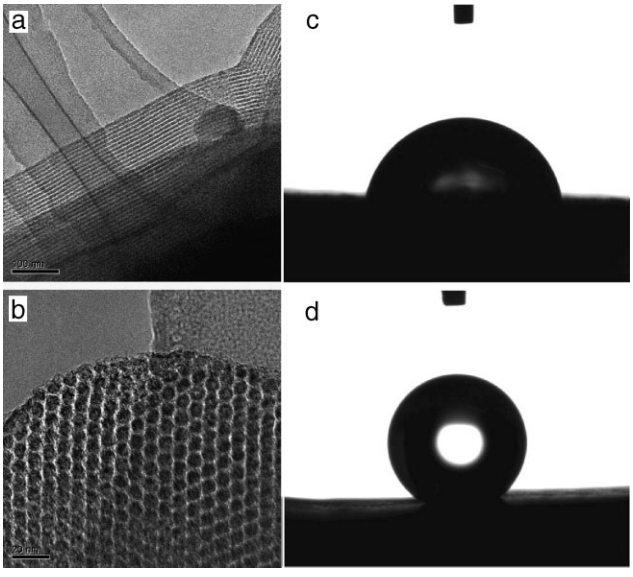


**Figure 4.** TEM images of a fluoroalkylsilane-treated porous carbon monolith in a) the [110] direction and b) the [100] direction. Photographs of water droplet shape on the mesoporous carbon monolith c) before and d) after modification of the surface with a fluoroalkylsilane. Reproduced with permission from Wang et al. [107]. Copyright Elsevier 2006.


WILEY InterScience DISCOVER SOMETHING GREAT
© 2008 WILEY-VCH Verlag GmbH & Co. KGaA, Weinheim

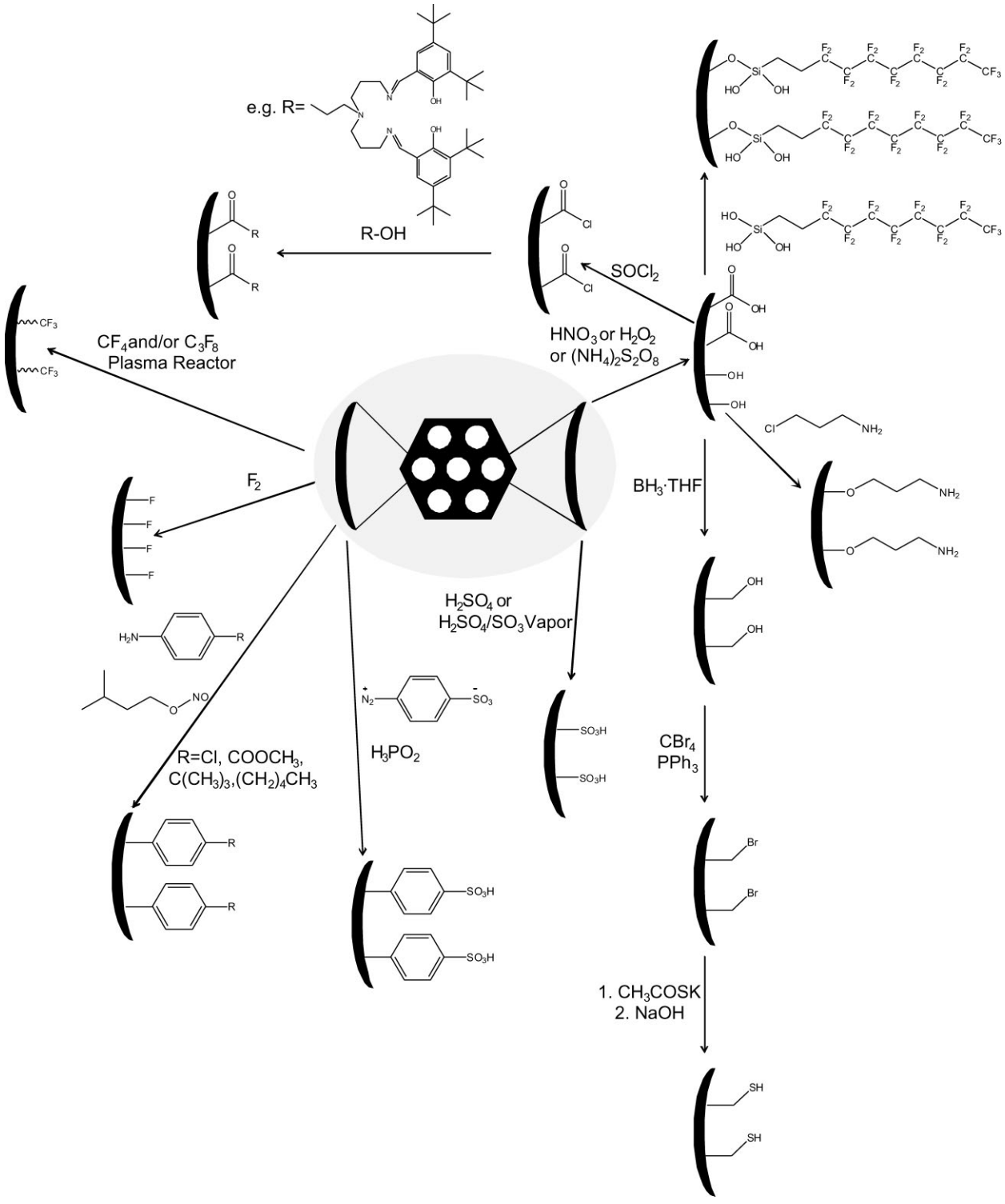


**Figure 5.** Summary of grafting reactions that permit functionalization of TNC surfaces with covalent anchors. Because the starting surfaces were not always fully specified in the original papers, idealized surfaces are depicted here. For more details, see the text and the original references.

and the surface functionality is changed by an organic reaction. In other methods, functional groups are attached directly to the carbon surface. In methods involving preexisting surface functionality, oxidation of the carbon surface with boiling nitric acid is a common choice, as noted above.[110,111]

*2.6.1. Attachment via Carboxyl Groups*

On mesoporous carbons CMK-1 and CMK-5, carboxyl groups generated by oxidation were reacted with thionyl chloride in order to convert them to acyl chloride groups.[110] The acyl chloride


© 2008 WILEY-VCH Verlag GmbH & Co. KGaA, Weinheim

groups could then be used to attach a Schiff-base ligand (3-(*N*,*N*′-bis-3-(3,5-di-*tert*-butylsalicylidenamino) propyl) hydroxypropylamine) onto the carbon surface by esterification. The Schiff base permits metal complexation. After complexation of $Mn^{2+}$ and oxidation to $Mn^{3+}$, the catalytic activity was investigated for the oxidation of cyclohexene with tetrabutylhydroperoxide. The catalytic activity was shown to be higher than that of a similar silica catalyst, and the porous carbon maintained order and catalytic activity after subjecting the catalyst to boiling water for 10 days, unlike the silica catalyst. The oxidized CMK-1 was also reacted with tetraethylenepentamine under reflux conditions to prepare a carbon material capable of metal chelation. The functionalized carbon was capable of adsorbing 0.4 mmol $Cu^{2+}$ per gram of carbon, while a similar silica system (MCM-41 functionalized with ethylenediamine) only adsorbed 0.1 mmol $Cu^{2+}$ per gram. Unfunctionalized carbon did not adsorb enough $Cu^{2+}$ to be detected.[110]

In another example, carboxyl groups on nitric-acid-treated 3DOM carbon were reduced to surface hydroxyl groups by refluxing in $BH_3 \cdot THF$. A variety of functional groups could then be generated. Hydroxyl groups were converted to bromine by reaction with $CBr_4$ and $PPh_3$. A thioester was then produced by reaction with $CH_3COSK$, which could be hydrolyzed to form thiol groups on the surface. This thiol-modified 3DOM carbon was tested for heavy metal adsorption and was capable of absorbing 0.2 mmol $Pb^{2+}$ per gram of carbon, while unfunctionalized carbon only absorbed 0.06 mmol $Pb^{2+}$ per gram of carbon.[111]

Modification of carbon with preexisting surface functionality can also be carried out on carbon that is synthesized with a large amount of oxygen-containing functional groups on the surface, such as the hydrothermal carbon mentioned earlier.[81] In that case, the hydrophilic carbon surface was functionalized with primary amine groups in one step by refluxing overnight in 3-chloropropylamine. The surface coverage of amine groups on the surface was greater than 4 mmol $g^{-1}$.

#### 2.6.2. Attachment via Diazonium Chemistry

Inasmuch as reactions with oxygen-containing functional groups have been shown to furnish high surface concentrations of a wide range of functional groups, reductive functionalization of carbon surfaces also provides a starting point for many different surface functionalities, while avoiding deterioration in mechanical strength and surface smoothness associated with carbon oxidation. Diazonium compounds have been used to directly functionalize the surface of porous carbon materials. The use of diazonium compounds to modify the surface of carbon materials was first demonstrated in 1992 for several types of carbon, including glassy carbon electrodes, carbon fibers, carbon powder, and highly ordered pyrolytic graphite (HOPG) electrodes.[112] A variety of diazonium salts, including 4-nitrophenyldiazonium tetrafluoroborate in an acetonitrile solution, were electrochemically reduced on the surface of the carbon. Other diazonium salts used include 4-cyano, 4-carboxyl, 4-benzoyl, 4-bromo, 4-(carboxymethyl), 4-acetamidobenzene, and 4-nitronaphthalene compounds. Surface coverages can be controlled more readily than in oxidative processes, merely by changing the solution concentration and electrolysis time.[112] Reduction can also be carried out non-electrochemically, using reducing agents such as isoamyl nitrite or hydrophosphorus acid.[113–116] A similar method was used for functionalization of porous carbon materials, including C15, CMK-5, and C48.[113,114] Substituted anilines (including 4-chloro, 4-*tert*-butyl, 4-butyl, or methyl-4-aminobenzoate) were mixed with the carbon and isoamyl nitrite. This process generated diazonium compounds in situ, which then reacted with the carbon surface. No additional solvent was necessary, and grafting densities of 0.9–1.5 μmol $m^{-2}$ were obtained. ''Greener'' solvent-free syntheses are also possible by employing ionic liquids with diazonium cations and noncoordinating, hydrophobic, floppy anions, such as *p*-butylbenzenediazonium bis(trifluoromethanesulfonyl)amidate. This ionic liquid was used to functionalize a carbon rod by electrochemical reduction and by thermal decomposition.[117] The surface density of functional groups was higher with electrochemical reduction (6.07 μmol $m^{-2}$) than with thermal decomposition (3.38 μmol $m^{-2}$).

#### 2.6.3. Functionalization by Prato's Reaction

Recently another interesting grafting approach based on Prato's reaction, the 1,3-dipolar cycloaddition of azomethine ylides, was described.[118] Ordered mesoporous carbon was heated in a solution containing the α-amino acid N-methylglycine and an aldehyde. The condensation product was attached to –C=C– double bonds via a cycloaddition reaction. This method permits simultaneous attachment of two different R-groups to the carbon surface, depending on the α-amino acid and aldehyde that are used. The mesostructure is maintained during the relatively mild reaction, and grafting densities in the range of ca. 0.22–0.72 mmol $g^{-1}$ are attainable. The success of the reaction depends on the local carbon structure and the availability of reactive edges on carbon sheets; functionalization of highly graphitic mesoporous carbon was unsuccessful by this method.

#### 2.6.4. Other Grafting Methods

Although the number of grafting studies involving ordered porous carbon materials is still relatively small, many other grafting techniques have been carried out on carbons without designed porosity. Because these techniques should also be applicable to TNCs, we will now list a few selected examples.

Besides functionalization with diazonium salts, electrochemical grafting on carbon is possible with diaryliodonium salts, a process which has been demonstrated for glassy carbon electrodes.[119] The electrodes were modified electrochemically by applying a potential 200 mV negative of the voltammetric peak for each respective salt. The functional groups attached by this method ranged from electron withdrawing to electron donating groups, and included nitro, carboxylic acid, bromine, chlorine, hydrogen, methyl and methoxy groups. While the surface coverage is approximately 25% lower for this method than with diazonium salts, the use of unsymmetrical salts allows for surface coverage with a mixture of two different aryl functional groups. Another suitable grafting process that has been demonstrated for glassy carbon involves electrochemical functionalization with 4-aminobenzoic acid.[120]

Several methods are available to produce an amine-functionalized carbon surface, which may be used to form subsequent amide linkages, hydrogen bonds, or merely to change the surface adsorption properties. Activated carbon treated with hydrogen to remove acidic functional groups was first nitrated by reaction of the carbon with acetic anhydride, sulfuric acid, and fuming nitric


WILEY InterScience DISCOVER SOMETHING GREAT
© 2008 WILEY-VCH Verlag GmbH & Co. KGaA, Weinheim

acid.[121] Subsequent reduction of the nitro groups to amino groups was carried out by reaction with ammonia and sodium hydrosulfite. Amination of the surface could also be accomplished by reaction with diamines.[122] After introduction of carboxylic groups onto the surface of activated carbon with nitric acid, the carboxylic acid groups were converted to the acid chloride by reaction with thionyl chloride, followed by reaction with a diamine (ethylene diamine or hexamethylenediamine). Activation with thionyl chloride resulted in more diamine being immobilized on the surface than reaction with nitric acid alone. It has also been shown that carbon fibers oxidized with nitric acid can be funtionalized with amine groups by reaction with tetraethylenepentamine. Both single- and double-bridged forms were present on the carbon surface.[123] 4-Nitrobenzene groups on carbon surfaces can be reduced to amino groups by refluxing the modified carbon with tin in hydrochloric acid.[116]

Acidic surface groups in activated phenolic carbons can be converted to basic surface groups (aromatic amine and pyridine groups) by high-temperature treatment with anhydrous ammonia.[124,125] Ammonia also acts as an etchant during this process. In case of activated carbon fibers, samples undergo weight loss while the nitrogen content, surface areas, micropore volumes, and micropore diameters increase. Direct activation of phenolic fiber precursors with ammonia is also possible. These treatments significantly enhance absorption of hydrogen chloride. The techniques should be directly applicable to TNCs.

Methods in which carbon materials are functionalized directly in one step have been developed. Activated carbon was reacted with alcohols, amines or thiols in solvent-free, microwave-assisted reactions in which organic groups were attached at double bonds. The conditions for the microwave reactions were quite moderate, with reaction times of less than 100 minutes at temperatures less than 200 °C.[126] Carbon black was directly modified in one step with phenyl, nitrophenyl and phenylazoaniline groups, by reaction with aniline precursors (aniline, 4-nitroaniline or 4-phenylazoaniline), sodium nitrite, and acid. The surface coverage (2.5 $\mu$mol m$^{-2}$ for nitrophenyl) was slightly higher than similar methods reported for porous carbons.[127] Although processing details for this reaction and the other grafting methods highlighted above may have to be altered for nanoporous carbons, these examples should provide good starting points for covalent functionalization of synthetic carbon materials with designed porosity.

Surface hydroxyl groups on carbon allow the material to be interfaced with silicates and other oxides. Activated carbon has been functionalized with vinyltrimethoxysilane (VTMOS), in order to render the carbon surface more hydrophobic. The surface of the activated carbon was first functionalized with hydroxyl groups, followed by reaction with VTMOS in toluene at an elevated temperature. The modified carbon adsorbed much less water, allowing more selective adsorption of volatile organic compounds.[128] In similar work, activated carbon was functionalized with VTMOS by soaking the carbon in a dilute aqueous solution of the alkoxide. This functionalization allowed better wetting of the carbon by propylene carbonate for use in electric double-layer capacitor applications.[129] A monolayer of oxygen-bridged Ti atoms was attached to a glassy carbon surface containing hydroxyl groups by reaction with a solution of $TiCl_4$ in hexane.[130]

Another effective method of covalently attaching functional groups to carbon surfaces involves a photochemical reaction of the carbon surface with an organic molecule bearing one or more alkene groups.[131] After treatment of carbon in a mild hydrogen plasma, the alkene is attached to the C–H terminated surface by extended UV exposure. In a recent demonstration of this method, trifluoracetic-acid-protected 10-aminodec-1-ene (TFAAD) was attached to a thin carbon film and used as an anchor for DNA oligonucleotides after removal of the protecting groups.[131] This mild method provides a stable, covalently bound interface, and works for both low-temperature and high-temperature forms of carbon. The method remains to be demonstrated on porous carbons, where UV absorption might prevent attachment in the interior of the sample, but it may be useful for thin porous carbon films and perhaps for selective functionalization of external TNC surfaces.

Finally, we should also mention the potential use of $\pi$-$\pi$ stacking interactions to modify surfaces of TNCs, a method that is quite effective in preparing carbon nanotubes or graphite for further functionalization.[132,133] Although this method provides noncovalent attachment at the immediate carbon surface, it has been used to secure complex structures, such as proteins, on sidewalls of carbon nanotubes, employing highly aromatic pyrenyl linkers, which interact strongly with carbon-nanotube side walls, or with the basal plane of graphite, via $\pi$-$\pi$ stacking. Graphene sheets present in TNCs should permit similar interactions.

### 2.7. Attachment of Nanoparticles

A wide variety of methodologies have been developed to functionalize carbonaceous materials by incorporating a secondary phase within carbon frameworks. These methods may be classified into three major groups, according to the type of secondary particles and the technique of incorporation: impregnation, metal-transfer reactions, and composite formation.

#### *2.7.1. Impregnation*

Incorporation of a secondary phase, commonly noncarbonaceous nanoparticles, into a porous carbon substrate could be defined as one method of carbon functionalization. The introduction of secondary nanoparticles further extends the applications of porous carbon systems and provides new features such as catalytic and electrochemical activities. Impregnation methods are widely used because they are relatively inexpensive and simple to carry out. Metal oxides, such as iron, copper, nickel, cobalt, manganese, zinc, and mixed metal oxides are formed within the mesopores of a carbon substrate after a series of steps, including wet impregnation, drying, and calcination.[134–139]

Since impregnation always involves contact between a precursor solution and the carbon surface, it is often necessary to perform some surface functionalization on the porous carbons to increase the hydrophilicity of the surface and guarantee efficient wetting of the TNC, in particular for aqueous precursors.[140] One example involves the generation of $MnO_2$ nanoparticles within ordered mesoporous carbon using a sonochemical reduction method.[141] The mesoporous carbon was first oxidized using $H_2SO_4$, which enhanced the hydrophilicity of the carbon surface. An aqueous solution of $KMnO_4$


© 2008 WILEY-VCH Verlag GmbH & Co. KGaA, Weinheim

was then introduced into the pores, and reduced to $MnO_2$ with the assistance of ultrasonic energy. A similar strategy was adopted to produce 1D $MnO_2$ nanowires confined within mesoporous carbon.[142] Alternatively, a hydrophobic solvent can be used to avoid such a premodification treatment. As an example, a porous carbon/Pt nanocomposite was prepared by impregnating a water-in-oil precursor into ordered mesoporous carbon following chemical reduction.[143] This strategy allowed good penetration of the precursor solution into the mesoporous carbon, which resulted in an even distribution of Pt nanoparticles throughout the material.

Porous carbon/tin dioxide nanocomposites are promising candidates as electrode materials for lithium-ion batteries. 3DOM C/$SnO_2$ was synthesized by a simple impregnation method.[21] An aqueous solution of $SnSO_4$ was introduced into an acid-treated 3DOM C monolith, followed by drying and thermal treatment to induce the decomposition of $SnSO_4$ to $SnO_2$. $SnO_2$ nanoparticles with diameters of 10–40 nm were produced evenly spread on the macropore walls of 3DOM carbon (Fig. 6). This composite exhibited higher lithium capacity and improved rate capability over bare 3DOM carbon. The incorporation of $SnO_2$ nanoparticles into small mesopores of ordered nanostructured carbon was achieved by impregnating $SnCl_2$ precursor with the assistance of $OP(OCH_3)$.[144] Here, instead of pretreating carbon to render the surface hydrophilic, an additive of hydrophobic $OP(OCH_3)$ was employed together with hydrophilic $SnCl_2$ to facilitate precursor impregnation and nanocomposite formation. Although deterioration of the ordered mesoporous carbon structure was observed after incorporation of the tin-based oxide, the composite showed improved cycleability compared to discrete $SnO_2$ nanoparticles.

Carbon-based composites containing precious metal oxides such as $RuO_2$ have recently become popular due to their high electrochemical performance as electrodes for capacitors. $RuO_2$ nanoparticles were generated within porous carbon networks by either sol–gel processes or impregnation methods.[145–147] A carbon/ruthenia composite was prepared by adding hydrous $RuO_2$ into a resorcinol-formaldehyde solution, followed by a polymerization process.[145] The mixture was then carbonized, and $RuO_2$ was reduced to Ru metal in situ by the carbon. The composite contained Ru nanoparticles with diameters of ca. 30 nm. These Ru nanoparticles were oxidized to hydrous ruthenium oxide, which is electrochemically active and contributed to the high capacitance of the composite. Since conventional activated carbons contain mostly micropores that are too narrow to be easily wetted by electrolytes, high-surface-area mesoporous carbons with more-accessible interconnected tunnels have drawn considerable interest. A chemical vapor impregnation method has been employed to incorporate ca. 3 nm Ru nanoparticles into the 12 nm pores of a mesoporous carbon.[147] The Ru loading could be controlled either by adjusting the mass ratio of precursor to carbon or by repeating the impregnation procedure. Although the total capacitance of the nanocomposite increased with Ru loading, the degree of Ru utilization for a pseudocapacitor became poorer, and the rate capability of the composite electrode decreased due to an increase in equivalent series resistance.

Another type of secondary functional phase consists of metallic nanoparticles. One of the systems that have attracted consider-

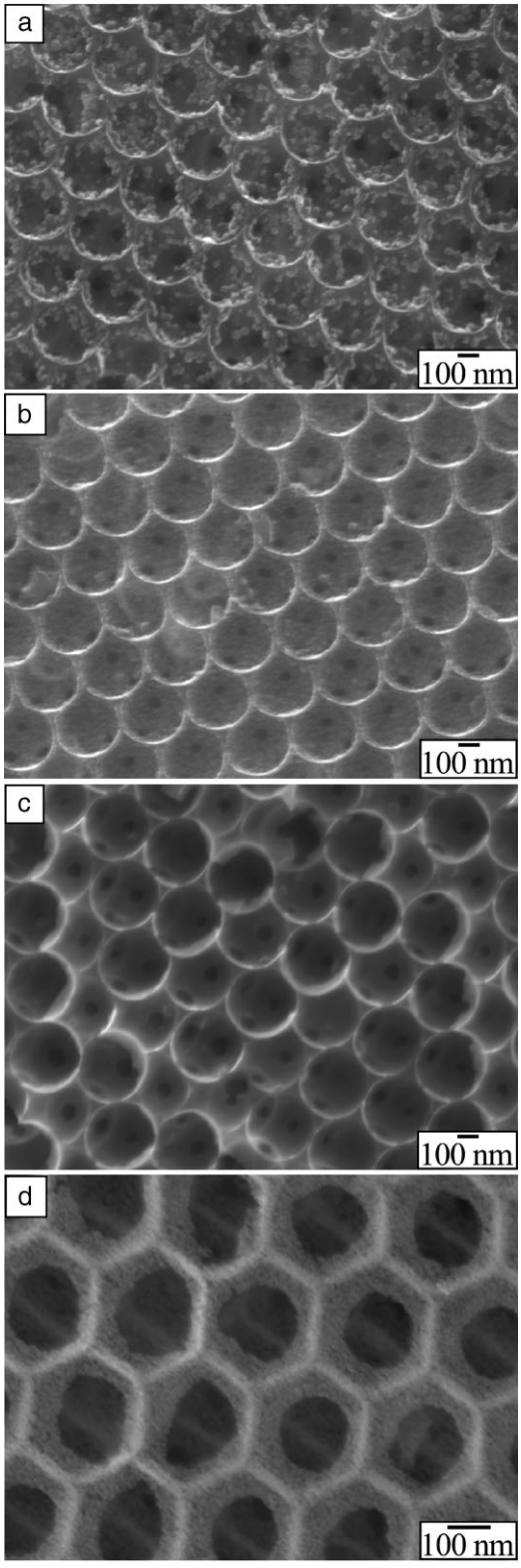


**Figure 6.** SEM images of a) 3DOM carbon after being impregnated with $SnSO_4$, b) after decomposition of $SnSO_4$ to form $SnO_2$, c) 3DOM C/$SnO_2$ after being cycled 30 times, and d) 3DOM $SnO_2$ obtained after heating the sample shown in b) at 900 °C in air. Reproduced with permission from Lee et al. [21].


WILEY InterScience DISCOVER SOMETHING GREAT
© 2008 WILEY-VCH Verlag GmbH & Co. KGaA, Weinheim

able interest during the past decade is the carbon/platinum nanocomposite. The combination of these two components brings together the advantages of high surface area of the porous carbon and unique catalytic functions of platinum, such as hydrogenation and electrochemical oxidation of hydrogen or methanol in fuel cell applications. Pt nanoparticles are typically loaded onto porous carbon via precursor impregnation followed by reduction with either hydrogen (under heat) or borohydrides.[143,148–154] The as-synthesized carbon/Pt materials have been studied extensively as oxygen reduction catalysts for direct-methanol fuel cells (DMFC). The conventionally adopted support for Pt is activated carbon, which contains mostly micropores. Therefore, Pt only covers the top surface of the support, and the interior porosity is not utilized efficiently. The high Pt loading on conventional carbon black severely limits its use as electrode in fuel cell applications. In addition, this surface-coating feature results in agglomeration of Pt after prolonged usage, which deteriorates the activity of the whole catalyst. Mesoporous carbons may overcome these limitations because their large, accessible pores can trap Pt nanoparticles while maintaining sufficient room for mass transport. In a pioneering study, platinum was introduced into ordered mesoporous carbon prepared by nanocasting from an SBA-15 template by an incipient-wetness and hydrogen-reduction procedure.[148] Highly dispersed Pt nanoparticles as small as 3 nm in diameter were obtained by this method. It was noted that by employing ordered mesoporous carbon as a support, Pt nanoparticles could be easily attained with both smaller size and narrower size distribution, compared to other types of support, such as carbon black, activated charcoal, and activated carbon fiber. Due to the high dispersion of Pt on ordered mesoporous carbon, significantly less platinum is required, which lowers the cost of the catalyst. The composite exhibited promising electrochemical activity toward oxygen reduction. Besides Pt, other metal species, such as Fe, Pd, Ni, and Ag have been loaded onto porous carbon substrates, introducing magnetic and/or catalytic properties to the systems.[140,155–160] Novel routes, such as surfactant-assisted microwave synthesis, have also been applied to produce Pt nanoparticles within mesoporous carbon.[161] The composite was evaluated as a hydrogen electro-oxidation catalyst, and results showed that the use of surfactants during the synthesis significantly improved the electrochemical activity of the catalyst.

#### 2.7.2. Metal Transfer Reactions

As an alternative to post-synthesis modification, a metal-transfer method may be used to introduce a metal component into a carbon framework.[162] This was demonstrated for a mesoporous Pt–alumina material that was synthesized by surfactant templating and calcined in an air or nitrogen stream. The product acted as the template for nanocasting with a divinylbenzene precursor. After carbonization and removal of alumina, Pt was left behind on the product, forming a carbon/Pt nanocomposite. Pt in samples synthesized from a mesoporous Pt-alumina template and calcined under a nitrogen stream was better dispersed than Pt loaded onto mesoporous carbon CMK-3 via a post-treatment method. This was attributed to the initial affinity of the Pt precursor to the alumina template, which restrained the growth of Pt species and led to the formation of fine Pt nanoparticles during the subsequent heating process. Better catalytic performance in methanol electro-oxidation experiments was demonstrated in the sample prepared from a template that was calcined in nitrogen rather than in air, corresponding to higher Pt dispersion in the former catalyst. These observations led to the suggestion that the Pt-loaded nanocomposites could be promising anode materials for DMFCs.

#### 2.7.3. Composite Formation

Metal precursors can be introduced with carbon precursors at the nanocasting stage to produce carbon-based nanocomposites with metals, such as cobalt, iron, and nickel.[163–165] During carbonization in an inert atmosphere, metal salts/oxides are spontaneously reduced to metal nanoparticles. In nanocasting syntheses using furfuryl alcohol and cobalt, nickel, or iron nitrate as precursors within mesoporous silica SBA-15, the metal nitrates acted as Lewis acids to catalyze the polymerization of furfuryl alcohol.[163] Subsequent carbonization under an inert atmosphere transformed the crosslinked polymer into a carbonaceous network. Metal nanoparticles were spontaneously generated and embedded within the mesostructured nanocomposites, after decomposition of the nitrates and reduction of the resulting metal oxides by carbon at a high temperature. Washing with NaOH solution removed the silica template and released the mesoporous carbon/metal composite. A fully protected Co-nanoparticle dispersion within mesoporous carbon could be obtained by a second addition of furfuryl alcohol before carbonization. The trapped cobalt resisted leaching with acid. A similar pathway of fabricating mesoporous carbon containing embedded magnetic nanoparticles was also developed using an iron salt and polypyrrole as precursors.[164]

Interestingly, carbon nanotubes were reported to grow on a mesoporous carbon/silica/Ni composite via CVD.[165] The carbon nanotubes acted as bridges connecting adjacent nanocomposite particles. After removal of silica and Ni from the system, mesoporous carbon bridged by carbon nanotubes was produced. The electric conductivity increased by a factor of five after incorporation of the carbon nanotubes. The cycleability of the carbon nanocomposite materials as an anode for a lithium-ion battery was improved. A flatter and more stable cycling curve was obtained for this novel composite, compared with pure ordered mesoporous carbon.

Recently, composites of mesoporous carbon with well-dispersed Ir or MoC clusters were synthesized by direct, one-pot methods, avoiding the need for a nanocasting mold, and produced smaller, more stable clusters than postimpregnation methods.[166,167] Salts of Ir or Mo were included in the resorcinol–formaldehyde surfactant mixture, and were reduced during pyrolysis. Under optimized conditions, the clusters did not disrupt the ordered carbon mesostructure.

### 2.8. Electrostatic Attachment of Nanoparticles

Nanoparticle attachment onto a porous substrate is yet another strategy of functionalizing porous carbon. A multistep functionalization method with nanoparticles is particularly useful for larger pores (macropores), as demonstrated for the synthesis of a 3DOM $C/TiO_2$ nanocomposite.[98] Three major stages are involved in this process: 1) chemical modification of the


© 2008 WILEY-VCH Verlag GmbH & Co. KGaA, Weinheim

3DOM carbon surface utilizing nitric acid, to introduce carboxyl groups that are further converted to negatively charged carboxylate groups; 2) fabrication of multilayer polyelectrolyte coatings via a layer-by-layer growth technique, using polymers with opposite charges and ensuring a positive charge on the outermost layer; 3) in situ attachment of negatively charged $TiO_2$ nanocrystals onto the carbon surface with the assistance of electrostatic attraction via hydrothermal reaction. As-synthesized samples exhibited a uniform coating of $TiO_2$ nanocrystals on the macropore wall of 3DOM carbon (Fig. 7). The coating quality and other parameters could be conveniently tuned by controlling the reaction temperature, precursor concentration, and reaction duration.

### 2.9. Polymer Surface Coating

By coating porous carbon surfaces with polymers, one can drastically alter its surface properties to modify its wettability, conductivity, and adsorption properties. Furthermore, through the formation of a porous carbon–polymer composite, the mechanical strength of the material is significantly enhanced, while the electronic conductivity of the carbon is maintained.[168]

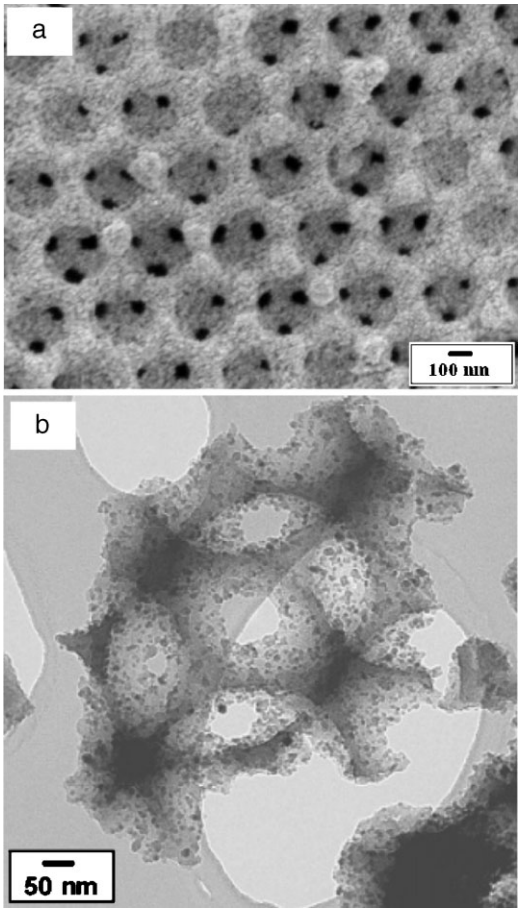


**Figure 7.** a) SEM and b) TEM images of 3DOM carbon coated with $TiO_2$ nanoparticles. Uniform dispersion of $TiO_2$ was achieved by the assistance of a layer-by-layer polyelectrolyte precoating, which enhanced the surface charge on 3DOM carbon. Reproduced with permission from Wang et al. [98]. Copyright American Chemical Society 2005.

With appropriate surface-coating methods, the porosity of the carbon support can be preserved, both for mesoporous and macroporous carbons. The following examples illustrate some of the methods used for modifying carbon surfaces with polymers and the effects of polymer addition on the structures and physical properties of the resulting nanocomposites.

One method for introducing polymers into mesoporous carbon is by wet impregnation with a solution containing suitable monomers, crosslinkers, and initiators. An early demonstration involved impregnation of the ordered mesoporous carbon, CMK-3, with a methylene chloride solution of styrene, divinylbenzene, and 2,2′-azobisisobutyronitrile.[168] If this mixture was heated without prior solvent removal, polymerization resulted in blockage of the mesopores. However, solvent evaporation followed by thermal polymerization in an inert atmosphere produced a carbon–polymer nanocomposite, in which mesopores remained accessible. It was proposed that micropores present in this carbon material were completely filled with organic monomers, and that mesopores were coated with a thin monomer layer, which was then converted to crosslinked polymers. The resulting interpenetrating composite framework exhibited high mechanical stability under compression. The electronic conductivity was lowered only minimally compared to the original carbon material, making the composite interesting for electrode applications, such as sensors and fuel-cell electrodes. In a similar study, in which polypyrrole was intercalated into hexagonal mesostructured carbon by wet impregnation of an ethanolic solution of pyrrole and ferric chloride as oxidizer, the framework structure experienced significant shrinkage.[169] Nonetheless, mesoporosity was maintained, and the electronic conductivity was only slightly reduced.

When the precursor for an ordered mesoporous carbon, i.e., the mesoporous silica–carbon composite, is functionalized with a polymer, the polymer does not intercalate the structure, but covers only the outside surface. Subsequent treatment with a HF solution removes the silica component, leaving ordered mesoporous carbon particles, each wrapped in a polymer shell. A recent study employed this method of surface-selective coating with polypyrrole to enhance the interfacial conductivity between carbon particles for a direct methanol fuel cell application, without relinquishing the high surface area and pore volume of the porous carbon.[170] The polypyrrole shell thickness was controllable via the polymerization time and the adsorption time of the monomer. Mesopores remained accessible, allowing their functionalization with highly dispersed Pt nanoparticles.

An interesting whiskerlike polymer structure was produced when polyaniline (PANI) was grown on the surface of mesoporous carbon with a concentration gradient of reagents between the inside and the outside of the mesopores.[171] Mesopores were first filled with an ethanol solution of aniline and $H_2SO_4$. The external solution was then quickly diluted and ammonium persulfate was added as an initiator. Because of diffusion limitations within the mesopores, the dilution proceeded more slowly in the pores than in the external solution. The resulting concentration gradient was thought to be responsible for initial precipitation of PANI at the pore openings, so that the growth pattern was related to the surface structure of the mesoporous sieve. The PANI ''nanothorn'' structure (10–20 nm diameters, 80–100 nm long, Fig. 8) was well suited to


WILEY InterScience DISCOVER SOMETHING GREAT

© 2008 WILEY-VCH Verlag GmbH & Co. KGaA, Weinheim

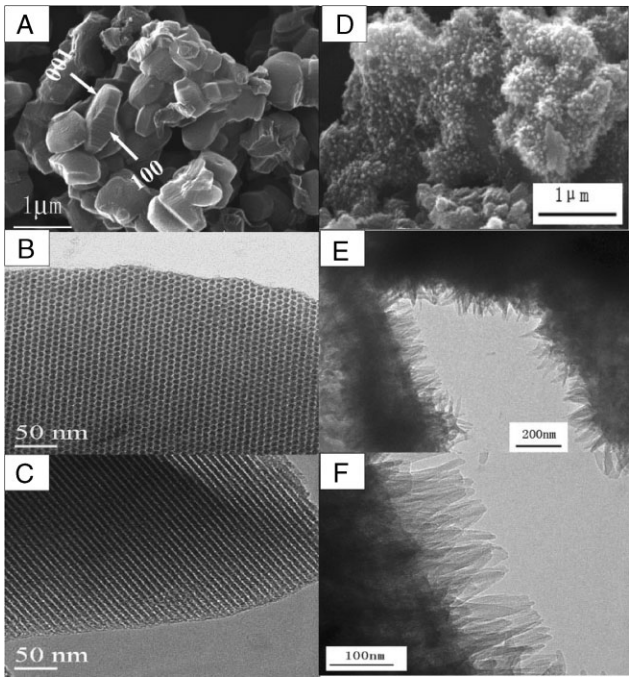


**Figure 8.** SEM and TEM images of mesoporous carbon (A, B, C) and PANI–mesoporous carbon composites (D, E, F). The PANI ''nanothorn'' structure is visible in E) and F). Reproduced with permission from Wang et al. [171].

enhance the specific capacity (1221 $F g^{-1}$) and high-rate charge–discharge ability of the composite, when employed as a supercapacitor electrode.

Because porous carbons are electronically conducting, their surfaces are amenable to coating by electropolymerization reactions. When a conductive polymer, such as polyaniline, is deposited on a porous carbon by an electrochemical synthesis, the coverage, thickness, and homogeneity of the coating depend strongly on the synthesis time.[172] Therefore, much optimization is needed to avoid plugging the pores. On the other hand, when a nonconducting polymer is deposited by electropolymerization, film formation occurs only as long as the conductive porous carbon surface remains accessible. As soon as the surface becomes insulated by a thin polymer coating, the reaction stops at that site. Hence, the reaction is self-limiting, and the resulting coatings are ultrathin, uniform, and conform to the internal surfaces of the porous carbon substrate. This has been demonstrated, for example, for ultrathin, electroactive poly(*o*-methoxyaniline) (POMA) coatings on carbon aerogels,[173] and subsequently for poly(phenylene oxide) (PPO) and sulfonated poly(phenylyne oxide) (SPPO) on 3DOM carbon surfaces.[174,175] In all these cases, the open pore architecture was largely retained after coating, and macropores remained accessible. For the POMA system, conformal growth was assured by working at a pH $> 1$, i.e., conditions where the polymer is insulating or poorly conductive. After deposition, the ca. 5 nm thin film could be made conductive again by choosing highly acidic electrolyte conditions.[173] In case of the PPO and SPPO systems, the polymer film coating the 3DOM carbon surfaces was estimated to be somewhat thicker (10–15 nm), and it was able to electronically insulate the carbon surface from a second interpenetrating electrode component, while permitting some lithium-ion transport across this membrane.[174,175] The PPO layer blocked micropores and mesopores in the 3DOM carbon electrode, reducing its specific surface area from 342 to 11 $m^2 g^{-1}$.

Polymer coatings can also be used to introduce positive or negative surface charges on porous carbon and increase the hydrophilicity of the modified carbon. This was demonstrated by coating a 3DOM carbon surface with multiple layers of positively and negatively charged polyelectrolytes (poly(diallyldimethylammonium chloride), PDDA, and poly(4-styrenesulfonate sodium), PSS, respectively).[98] This layer-by-layer growth required initial oxidation of the carbon surface, to produce a small negative surface charge and attract the first PDDA layer. Similar to the case of electrodeposited PPO, the surface area decreased from more than 400 $m^2 g^{-1}$ for $HNO_3$-treated 3DOM carbon to only 17 $m^2 g^{-1}$ for polyelectrolyte-coated 3DOM carbon, which corresponds approximately to the theoretical value for a smooth, inverse-opal surface lacking any additional porosity. This indicates a conformal and dense coating of polyelectrolyte layers on the carbon surface. Hence, this technique could be a promising method for controlling the porosity and surface texture. After the carbon surface had been coated with multiple layers of alternating charge, it provided a convenient substrate for confined growth of nanoparticles (see discussion above).

Finally, grafting of polymers to or from porous carbon surfaces is a viable method of modifying their surface chemistry. Methods of grafting polymers to carbon materials such as nanotubes, graphite powder, fibers, and carbon black are fairly well established.[69,71] ''Grafting to'' involves attaching hydroxyl- or amine-terminated polymers to active groups on the carbon surface, such as carboxyl, acyl chloride, acyl azide, and epoxide groups. A wide variety of traditional polymers can be attached using this method, and attachment of biological moieties such as DNA and proteins is also possible. ''Grafting from'' is a related method in which an active group is attached to the carbon surface, and is used to initiate polymerization. Using this method, various initiating groups such as azo, peroxyester, potassium carboxylate, and acylium perchlorate groups can be used to initiate anionic, cationic, and radical polymerizations of many different monomers. Although not yet widely studied for nanoporous carbons, ''grafting from'' methods would probably be more suitable for mesoporous carbons with limited accessible pore spaces, while ''grafting to'' should be applicable for macroporous carbons, which have sufficient room for postsynthesis introduction of preformed polymers. Previously, it has been demonstrated that mesoporous silica can be employed as an extrusion host for the synthesis of polyethylene nanofibers.[176] Given their comparatively high mechanical and chemical stability, nanoporous carbons may similarly prove to become useful reactors for polymerization of nanofibers and other processes.

## 3. Characterization

The bulk elemental composition of typical designed carbon materials is relatively easily determined by CHNS analysis, based on the classical Pregl-Dumas method. Commercial instruments are


© 2008 WILEY-VCH Verlag GmbH & Co. KGaA, Weinheim

available for routine analysis, in which samples are combusted completely in a pure oxygen environment and reduced to the elemental gases $CO_2$, $H_2O$, $N_2$, and $SO_2$. These gases are then separated by frontal chromatography and analyzed. More specific identification of functional groups requires an array of spectroscopic and nonspectroscopic techniques, which are outlined below. Data interpretation is often not straightforward for carbon materials, due to the convolution of contributions from different functional groups.[177] Here, we will highlight techniques for characterizing the bulk, external surface, and internal surface of carbonaceous samples, with an emphasis on functional group analysis. This section is by no means a comprehensive review, but is aimed at helping the reader choose appropriate analytical techniques.

### 3.1. Bulk Characterization

#### *3.1.1. Solid-State NMR*

Solid-state NMR spectroscopy, a widely used technique to monitor functionalization of porous silica materials, has not yet been employed as frequently for analyses of functionalized carbon materials with designed pore structures. However, high-resolution solid-state $^{13}C$ NMR spectroscopy is well established for analyses of coals and activated carbons,[178] and many of the approaches that have been developed for those types of carbons also lend themselves to the study of structural changes of periodic mesoporous or macroporous carbons, before and after surface functionalization. Owing to the complexity of many carbonaceous structures, the chemical shift ranges for various functional groups are not always clearly defined, and overlap is common.[105] However, complex carbonaceous structures can be analyzed in detail by combining data from multiple solid state NMR techniques.[179] $^{13}C$ cross-polarization magic-angle-spinning (CP-MAS) NMR experiments provide qualitative information about the structure of carbonaceous solids, revealing, for example, aromatic and aliphatic resonances.[180] Due to differences in the rates of polarization transfer from $^1H$ to $^{13}C$ spins between different types of carbon atoms, careful selection of contact times is required for CP experiments. Even then, a substantial fraction of carbon atoms might not be observed.[181] Spinning sidebands that overlap with the carbon resonances should be avoided using sideband suppression techniques.[179] Dipolar dephasing experiments and $^{13}C$ CP-MAS spectral editing techniques provide accurate information about ratios of protonated and nonprotonated aromatic and aliphatic carbons, respectively.[179] Detailed information about the aromatic region of a sample is accessible by isotropic–anisotropic correlation experiments.[179] More quantitative $^{13}C$ MAS NMR determinations of carbon functional groups require single-pulse experiments with large-volume rotors and very long delay times, for carbon magnetization to recover to its full thermal equilibrium value (ca. 5 times the $^{13}C$ $T_1$ relaxation time). Because $T_1$ for carbon materials itself can be very long, such measurements are extremely time intensive.[182] If the carbon sample contains significant amounts of oxygen, the relaxation time may be shorter. For porous carbon samples with high surface areas, adsorbed oxygen can also act as a source of relaxation.

Some $^{13}C$ NMR studies related to designed porous carbons include an investigation of the phenol–formaldehyde resin precursors,[183] porous carbon nanospheres,[184] zeolite-templated, furfuryl alcohol-based microporous carbons,[185] and mesoporous carbon CMK-3 samples before and after sulfonation.[105] Other useful NMR-active nuclei to study the functionalization of porous carbons include $^1H$, $^{15}N$, and $^{19}F$. $^1H$ solid-state NMR of carbonaceous solids is complicated by the high abundance of protons in many of these materials. It is therefore necessary to use $^1H$ NMR techniques that eliminate the effects of $^1H$–$^1H$ dipolar interactions that lead to strong line broadening, for example combined rotation and multiple-pulse spectroscopy (CRAMPS).[186] $^{15}N$ NMR experiments need to address the opposite challenge: low natural abundance, a negative gyromagnetic ratio, and 50-times lower sensitivity than $^{13}C$. Nonetheless, $^{15}N$ CP-MAS NMR spectroscopy has been successfully applied to determine nitrogen functional groups (pyrroles, indoles, carbazoles, pyridines, amides, imides, imines, and nitrile functionalities) in carbon samples, though with only modest signal-to-noise ratios.[182,187] Sample heterogeneity can result in different cross-polarization dynamics for different types of nitrogen functional groups, specifically when comparing nitrogen compounds with and without directly bonded protons. $^{19}F$ solid-state NMR has been applied to follow fluorination processes in nanocast porous carbon samples.[188] Because of the high nuclear sensitivity and isotopic abundance of the $^{19}F$ nucleus, a sensitive technique for determining different oxygen functionalities in carbonaceous species involves $^{19}F$ MAS NMR after fluorination of the sample with diethylaminosulfur trifluoride.[189] Although it has not yet been applied to mesoporous carbons, this method was used for the analysis of coal, and allowed detection of functional groups (primary and secondary fluorides, aromatic and aliphatic carboxylic acid fluorides, primary and secondary alcohol groups) at the part-per-thousand level.

#### *3.1.2. Fourier-Transform (FT) IR and Raman Spectroscopy*

FT-IR spectroscopy has been used to determine functional groups on coals, carbon blacks, chars, and activated carbon structures,[89] and it is also suitable for investigations of synthetic porous carbons.[98] To evaluate the success of carbon surface functionalization, it is expedient to compare spectra of nonfunctionalized and functionalized materials, and follow the appearance and disappearance of absorption bands. Spectra are often only of modest quality, exhibiting low signal-to-noise ratios and distinct background features. These effects arise from the poor transmission of carbon, which is caused by its strong electronic absorption and by light scattering effects.[190] To minimize uneven light scattering, samples should be ground to the smallest possible particle size, while taking care not to contaminate the sample or cause it to oxidize due to local hot spots during grinding.[89] When samples are dispersed in KBr pellets, ion exchange with the KBr must be avoided, when the pellet is pressed.[190] Specialized techniques that can improve the spectral quality include attenuated total reflectance (ATR, if good contact can be made between the ATR windows and the sample) and diffuse reflectance (DRIFTS) methods. Photoacoustic spectroscopy has also been used with carbon samples, though not widely.[190] In situ DRIFTS measurements have been used to study the formation of surface groups on carbon by oxidation.[87,177] Cyclic ethers, cyclic anhydrides, lactones, quinones, ethers, and phenols were among the groups identified by this


WILEY InterScience DISCOVER SOMETHING GREAT

© 2008 WILEY-VCH Verlag GmbH & Co. KGaA, Weinheim

**Table 1.** Infrared vibrations of functional groups on carbon surfaces. Data have been taken from Fanning et al. [87], Zawadski [89], and Painter et al. [190].

| Functional Group | Assignment Region [$cm^{-1}$] |
|---|---|
| C–O stretch of ethers | 1000–1300 |
| Ether bridge between rings | 1230–1250 |
| Cyclic ethers containing COCOC groups | 1025–1141 |
| Alcohols | 1049–1276, 3200–3640 C–OH stretch: 1000–1220 |
| Phenolic groups | O–H bend/stretch: 1160–1200, 2500–3620 |
| Carbonates; carboxyl-carbonates | 1100–1500, 1590–1600 |
| Aromatic C=C stretching | 1585–1600 |
| Quinones | 1550–1680 |
| Carboylic acids (COOH) | 1120–1200, 1665–1760, 2500–3300 |
| Lactones | 1160–1370, 1675–1790 |
| Anhydrides | 980–1300, 1740–1880 |
| Ketenes (C=C=O) | 2080–2200 |
| C–H stretch | 2600–3000 |
| Amides | 1400–1420, 1620, 1660 |
| Amines | 3200–3400 |

spectroscopic method. Several other functional groups that can be determined by FT-IR spectroscopy are listed in Table 1, together with the positions of the corresponding IR absortions (see also Fig. 2).

Raman spectroscopy is a technique complementary to FT-IR, as some IR-inactive vibrations can be active in Raman spectra of carbonaceous materials. Most Raman studies of synthetic porous carbons have been limited to determining the degree of graphitic carbon versus disordered carbon, on the basis of the $E_{2g}$ and D bands near 1580–1620 and 1340–1350 $cm^{-1}$, respectively,[34,191–193] or perhaps to identifying spectral features near 310 $cm^{-1}$, related to a single-wall carbon structure of nanoscale curvature.[194]

### 3.2. External Surfaces

#### *3.2.1. X-ray Photoelectron Spectroscopy (XPS)*

In templated carbons, XPS can provide valuable information about the presence and amount of nitrogen groups, carbon groups, oxygen, fluorine, sodium, and other components.[177,195,196] Using this technique, it is possible to follow the development of functional groups with temperature[196] or to detect carbon–fluorine groups that may be produced on the surface of ordered mesoporous carbon by dissolution of the silica template with HF.[195] Silica remaining from an incompletely dissolved template after nanocasting may also be observed by XPS. Table 2 lists the binding energies for representative functional groups on carbonaceous materials. When XPS is applied to characterize the composition of designed porous materials, it must be kept in mind that this surface technique provides a compositional estimate of only the outermost layers, with a penetration depth of ca. 5–15 nm.[177,195] In typical ordered mesoporous carbon materials, most of the surface is located in mesopores, requiring additional analytical techniques.

**Table 2.** Binding energies of representative functional groups on carbonaceous materials. Data have been taken from Weidenthaler et al. [196], Darmstadt et al. [195], and Figueredo et al. [177].

| Atom | Functional Group | Binding Energy [eV] |
|---|---|---|
| N 1s | Pyridine | 398.0 |
| | Pyrrole | 399.2–399.9 |
| | Pyridone | 399.2–400.7 |
| | Quaternary nitrogen in pyridinium or ammonium species in graphene layers | 400.7 |
| | Pyridine-*N*-oxide | 402.5-403.8 |
| C 1s | C=C $sp^2$ | 284.7 |
| | C=N | 286.0 |
| | C=O | 287.2–287.4 |
| | COOH | 288.4–289.9 |
| | C–C | 284.6 |
| | C–O | 286.1 |
| | C–OH | 285.9 |
| O 1s | Quinone, carbonyl oxygen | 531.1 |
| | Lactone (C=O), phenol, ether | 532.3 |
| | C–OH | 532.8 |
| | Anhydride or H-bonded ketone | 533.3 |
| | Carboxylic acid | 534.2 |
| | Chemisorbed water | 535.9 |
| | Adsorbed oxygen | 537.6 |

#### *3.2.2. Secondary-Ion Mass Spectroscopy (SIMS)*

An even more surface-selective analytical method is SIMS. In this technique, the surface of the sample is bombarded with high-energy ions, which cause ejection of ions and neutral species whose identity depends on the nature of the surface functional groups. Static SIMS probes only the first atomic layer (the true surface region), whereas XPS probes slightly deeper into the near-surface region. For ordered mesoporous carbons, the SIMS spectra depend strongly on the sample history, including pyrolysis and postpyrolysis heat treatments.[195] By combining SIMS measurements with XPS data, it was determined that the outer surface of mesoporous carbon molecular sieves has a graphite-like, polyaromatic character.[197]

### 3.3. Internal Surfaces

#### *3.3.1. Chemical Titration*

Accessible acidic and basic sites on the surface of porous carbons are amenable to characterization by acid-base depletion and chemical titration.[89,98,109,198,199] Oxygen-containing groups, like ketones, phenols, lactones, lactol, carboxylic acids, and carboxylic anhydrides, can be categorized by wetting and equilibrating the carbon samples with a range of standard base solutions ($NaOC_2H_5$, NaOH, $Na_2CO_3$, and $NaHCO_3$), and then back-titrating the bases with a standard strong acid. The acid dissociation constants of carboxyl groups, lactones, or phenols differ by several orders of magnitude.[109] One can therefore extract $pK_a$ and $pK_b$ values from the titration data.[199] Mass titration or electrophoresis may be used to determine isoelectric points and surface charges of the carbon samples.[109] Calorimetric measurements of heats of neutralization can supplement this information.[199] Functional groups buried within the pore


© 2008 WILEY-VCH Verlag GmbH & Co. KGaA, Weinheim

walls are not detected by these methods. Titration is most useful when applied in combination with other techniques, such as FT-IR spectroscopy. To determine the content of OH and NH groups, for example, acetylation reactions with acetic anhydride introduce strongly absorbing ester or amide bands with well-established group frequencies into the sample spectrum.[190] Carboxylic acid groups may also be confirmed by classical chemical-detection methods, including esterification with methanol or formation of acyl chlorides with thionyl chloride.[109] Redox titrations (e.g., with $Ce^{IV}$ solutions) allow detection of reducing groups that may have been introduced into the porous carbon during thermal treatment under reducing conditions.[200]

### 3.3.2. Electrochemical Techniques

Electrochemical techniques are highly surface sensitive, and have been used in order to assess surface functionalities of porous carbon materials.[201,202] Useful information is obtained from both galvanostatic and voltammetric methods. The redox behavior of surface oxygen complexes (hydroxyl, carbonyl, or quinone groups) is charactized by cyclic voltammetry (CV), a technique capable of differentiating between CO-type groups and carboxylic anhydrides. Surface oxygen groups can enhance the capacitance of carbon based on redox mechanisms (pseudocapacitance). They also affect the formation and structure of the double layer. In addition, oxygen groups play an important role in determining wettability of the porous carbon by an electrolyte solution.

### 3.3.3. Temperature-Programmed Desorption (TPD) and Reduction (TPR)

Surface groups that decompose at specific temperatures to form gas-phase products can be characterized by TPD experiments, for example, using a differential scanning calorimeter and a thermogravimetric analyzer (DSC-TGA) coupled to a mass spectrometer.[199] Oxide-containing functional groups decompose in specific temperature ranges to produce CO, $CO_2$, or $H_2O$ as decomposition products (see Table 3). Relative concentrations of surface oxides can then be estimated by deconvolution from the total amounts of these gases, which thermally desorb from the carbon sample.[177,199,201] Activation energies for the decomposition of surface groups may be calculated from the measured decomposition rates.[203] TPR is an analogous technique to study the reactivity of surface functional groups upon sample heating in a reductive atmosphere.[204] Hydrogen gas reduces surface complexes, which can then desorb, leaving active carbon sites for further reaction with hydrogen. For example if nitrogen groups are present in the sample, the evolution of $NH_3$, HCN, NO, and $N_2$ can be monitored as a function of temperature. It is possible to deduce the identity and quantity of original surface groups from correlated TPR and TPD data.[204]

**Table 3.** Determination of functional groups on carbon by TPD. Adapted from Tremblay et al. [203] and Figueiredo et al. [177].

| Functional Groups | Decomposition Products | Reported Decomposition Temperatures or Ranges [K]* |
|---|---|---|
| carbonyl | CO | 973–1253, 1073–1173 |
| quinone | CO | 973–1253, 1073–1173 |
| ether | CO | 973 |
| carboxylic anhydride | CO, $CO_2$ | 623–673, 873, 900 |
| lactone | $CO_2$ | 463–923, 623–673, 900 |
| lactol | $CO_2$, $H_2O$ | nr |
| carboxylic acid | $CO_2$, $H_2O$ | 373–673, 473–523 |
| phenol (hydroxyl) | CO, $H_2O$ | 873–973 |
| hydroquinone | CO, $H_2O$ | nr |
| aldehyde | CO, $H_2O$ | nr |

* nr = not reported in these references

### 3.3.4. Gas Sorption Isotherms

Gas ($N_2$, $CO_2$, Ar, etc.) sorption measurements are usually carried out for the determination of pore texture, such as pore-size distributions, pore volumes, and surface areas.[205,206] In mesoporous carbons, specific surface areas are calculated by application of the BET method to nitrogen adsorption isotherms. Total pore volumes may be calculated by a single-point measurement at a high relative gas pressure ($p/p_0 = 0.98$), micropore volumes by applying the Dubinin-Radushkevich analysis on the isotherm in a low relative pressure range ($10^{-4}$ to $10^{-2}$), and volumes of pores $<1$ nm by the Horvath-Kawazoe (HK) method applied to the relative pressure range from $10^{-6}$ to $10^{-4}$.[100] For evaluation of the pore size range $<0.7$ nm (ultramicropores), $CO_2$ adsorption at 0 °C is most useful, because the higher adsorption temperature compared to $N_2$ results in better diffusion of the gas molecules in these small pores.[207] Mesopore volumes are then determined by the difference between total pore volumes and micropore volumes. Mesopore- and micropore-size distributions are established by the Barrett–Joyner–Halenda (BJH) and HK methods. For mesoporous solids with cylindrical mesopores, pore-size distribution curves are improved by the Kruk-Jaroniec-Sayari (KJS) method, which combines BJH analyses with information about the statistical film thickness curves (t-curves) for argon and nitrogen on the specific support surface.[208–210] This method, which was first developed for mesoporous silicates, has recently been extended to nitrogen- and argon-sorption isotherms of carbonaceous materials with cylindrical mesopores in the pore-size range from 1 to 12 nm.[211] For nanoporous materials with regular spherical cages, nonlocal density functional theory (NLDFT) provides very good estimates of pore dimensions.[212] By comparing textural properties of samples before and after functionalization, one can infer about the presence and location of functional groups, although complications may arise from specific gas interactions with the carbon surface or the functional groups. It has been pointed out, for example, that at low pressures, when less than a monolayer of nitrogen has formed on the surface, the shape of the nitrogen adsorption isotherm (i.e., the position of the monolayer formation peak) depends on the graphitic character of the surface.[195] For mesoporous carbons, it is useful to compare potential changes in pore dimensions with small-angle data from powder X-ray diffraction to detect structural shrinkage that may also have occurred as a result of surface functionalization.

### 3.3.5. Wettability

The wettability of internal surfaces can be studied by gravimetric solvent-uptake experiments, using solvents of different polarities. Changes in wettability and surface polarity after functionalization of external surfaces are conveniently determined by contact-angle


WILEY InterScience DISCOVER SOMETHING GREAT

© 2008 WILEY-VCH Verlag GmbH & Co. KGaA, Weinheim

measurements.[108] Measurements of contact angles for at least two standard reference liquids with significantly different polarities can be used to derive total surface energies and their polar and dispersive components.[93]

*3.3.6. X-Ray Diffraction and Small-Angle X-Ray Scattering*

Diffraction techniques are most useful for determining mesostructural periodicity, pore geometry, and unit cell parameters of mesoporous carbons. However, some information regarding successful filling of pores with functional groups can also be derived from X-ray diffraction data, by analyzing relative peak intensities before and after surface functionalization. When mesopores are filled by modifying species, and the electron density of the pore content closely matches that of the pore walls, peaks related to the mesostructure decrease in intensity. No such changes occur if only the external particle surface is modified. These phenomena are well known for mesoporous silica systems,[213] but also apply to mesoporous carbon. However, in the interpretation of the data, structural deterioration must be considered as a possible alternate cause for reduced intensities. The data should therefore be interpreted in parallel with transmission electon microscopy (TEM) analysis.

*3.3.7. Imaging Methods*

Imaging of functional groups in porous carbon samples by TEM or scanning electron microscopy (SEM) is applicable only if such modifiers are suffiently large to be resolved (e.g., attached nanoparticles),[98] and for TEM if they provide sufficient contrast compared to the carbon background (e.g., metallic clusters).[150] Staining of functional groups (e.g., gold clusters to show thiol-groups) can help locate the functional groups and evaluate their distribution across the carbon support. By combining microscopy with energy-disperse spectroscopy (EDS) and electron-energy-loss spectroscopy (EELS), it is possible to map out the chemical composition of the sample averaged over the area exposed to the electron beam. Because of the high degree of overlap of carbon walls in a porous skeleton, and potential variations in the thickness of these carbon walls, great care must be taken in the interpretation of microscopy images. Electron tomography can aid the image analysis process.[214]

## 4. Applications

Due to their chemical stability, electronic conductivity, ability to intercalate electrochemically active species, and sorption capabilities, nanostructured carbons are interesting materials for a range of applications related to energy storage, sensing, catalysis, and sorption. Many of these applications have previously benefited from other forms of carbon, including glassy carbon and graphitic carbon for electrodes and activated carbons for catalysis and sorption. However, the new carbon materials with designed porosity can provide signicant benefits related to tunable surface areas, pore-size distribution, and pore access. Even more advantages can be derived by modifying the carbon wall or surface composition. In this section we will highlight applications of mesoporous and macroporous carbons with a particular emphasis on the effects of carbon functionalization on each application. Some examples also involve more traditional carbons, when they can provide direction for future studies involving designer carbons.

### 4.1. Sensors

Porous carbons, especially those with large pore volumes, are suitable for sensor substrates for several reasons, including electrical conductivity and large surface areas. A mesoporous carbon foam (MSU-F-C) was used as an immobilization host for glucose oxidase (GOx).[215] A higher loading of GOx ($(39.1 \pm 0.7)$ wt %) was achieved for this carbon than for graphite, activated carbon, and mesoporous carbon CMK-3, mainly due to the large pores of MSU-F-C. To employ the mesoporous carbon as a glucose sensor, MSU-F-C was combined with Nafion and coated onto a glassy-carbon electrode, followed by immobilization of GOx. This sensor exhibited high sensitivity as well as fast glucose response (Fig. 9). 3DOM carbon was also used in a sensor system, as the solid contact in a solid-contact ion-selective electrode (SC-ISE).[216] In this system, the carbon was attached to a metal current collector, and covered with a poly(vinyl chloride) sensing membrane containing ionophore and ionic sites. The sensor was selective for $K^+$, had a detection limit of $10^{-6.2}$ M, showed excellent long-term stability, and was resistant to interferences from $O_2$ and light; in contrast to semiconducting polymers, which have been used as solid-contact materials and have shown light interference. A similar SC-ISE based on 3DOM carbon as the

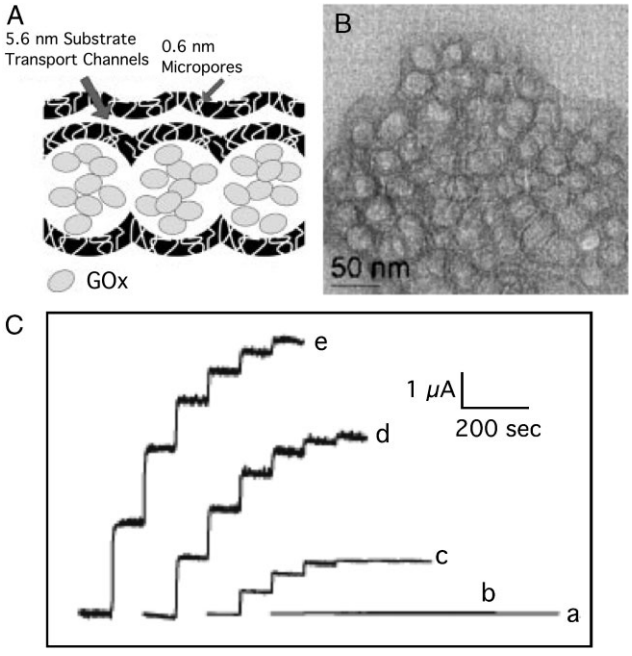


**Figure 9.** A) Schematic representation of an MSU-F-C/glucose oxidase composite, showing effective retention of enzymes within large mesopores and the role of small pores in the facile transport of a substrate. B) TEM image of MSU-F-C. C) Current response of the glucose biosensor prepared with different MSU-F-C contents on successive additions of 1 M glucose aliquots (10 μL each). The MSU-F-C contents are: a) 0, b) 0.5, c) 1.0, d) 2.0, and e) 3.0 $mg \cdot mL^{-1}$ in Nafion solution. Reproduced with permission from Lee et al. [215].


© 2008 WILEY-VCH Verlag GmbH & Co. KGaA, Weinheim

solid contact displayed an impressive sub-nanomolar detection limit for $Ag^+$.[217]

#### 4.2. Li-Ion Batteries

Carbon materials, especially graphite, have been investigated for lithium-ion battery anode materials for quite some time, due to their ability to intercalate lithium ions. Recently, porous carbons have gained interest as anode materials. Even without further functionalization, mesoporous carbons can have large capacities, larger than those of some other carbon materials, including some carbon nanotube systems. Because of their high surface areas, they exhibit large capacity losses in the first cycle, due to electrolyte decomposition at the carbon surface. But the high surface areas and porous structures also enhance lithium-ion transfer. Hence, these materials appear to be useful for situations where quick charge and discharge are desired. C-FDU-5 demonstrated a reversible capacity of 131 mAh $g^{-1}$.[218] CMK-5 gave charge capacities between 525 and 600 mAh $g^{-1}$ during the first three cycles.[219] Cyclic voltammetry showed that intercalated lithium was removed uniformly during deintercalation. The ordered mesoporous carbon CMK-3 exhibited a very high reversible capacity (up to 1100 mAh $g^{-1}$) and good cycle performance.[220]

The performance of the electrode can be altered through composite formation. Mesoporous carbon CMK-3 served as a substrate for an ordered, nanostructured tin-oxide–carbon composite (ONTC), in which tin-based oxides were deposited into the pores of the carbon.[144] For comparison, nano-$SnO_2$ (templated with the surfactant P123) and nano-MTBO (mixed tin oxides templated with P123) were examined. The initial charge capacity for nano-MTBO was slightly higher than that of ONTC, probably due to the smaller surface area of ONTC. However, the discharge capacity of ONTC was higher, and the irreversible capacity loss was high for both. The capacity fade for ONTC was smaller than either of the other two materials, with a capacity retention of 42.8%. The higher reversible capacity was probably due to the carbon template, which helped prevent large volume changes of the tin oxides and aggregation of the Li-Sn alloys, and provided an electrical contact between the tin composites.

To help overcome the poor cyclablity of $SnO_2$ due to large volume changes, hollow carbon spheres were synthesized by CVD deposition of carbon onto silica spheres followed by silica removal (Fig. 10).[221] The crystalline hollow carbon spheres were subsequently decorated with $SnO_2$, and upon carbon removal, hollow $SnO_2$ spheres were produced. Electrodes of carbon spheres, $SnO_2$-modified carbon spheres, and $SnO_2$ spheres were compared. The hollow carbon spheres showed good rate capability and cyclability. The carbon/$SnO_2$ particles showed a higher specific capacity, and did not have the loss of cyclability often seen for $SnO_2$ materials. The $SnO_2$ spheres had a specific capacity higher than the theoretical value of $SnO_2$, possible due to lithium storage within micropores between spheres or in the cavities of the hollow spheres. The promising properties of these materials are attributed to the crystallinity of the carbon spheres and to their hollow structure, which allows for high surface area, short diffusion pathlengths, and recapture of $SnO_2$ particles that detach from the inside of the spheres. Similar experiments showed that nitrogen-doped hollow carbon spheres performed better at higher current rates than undoped hollow carbon spheres.[222]

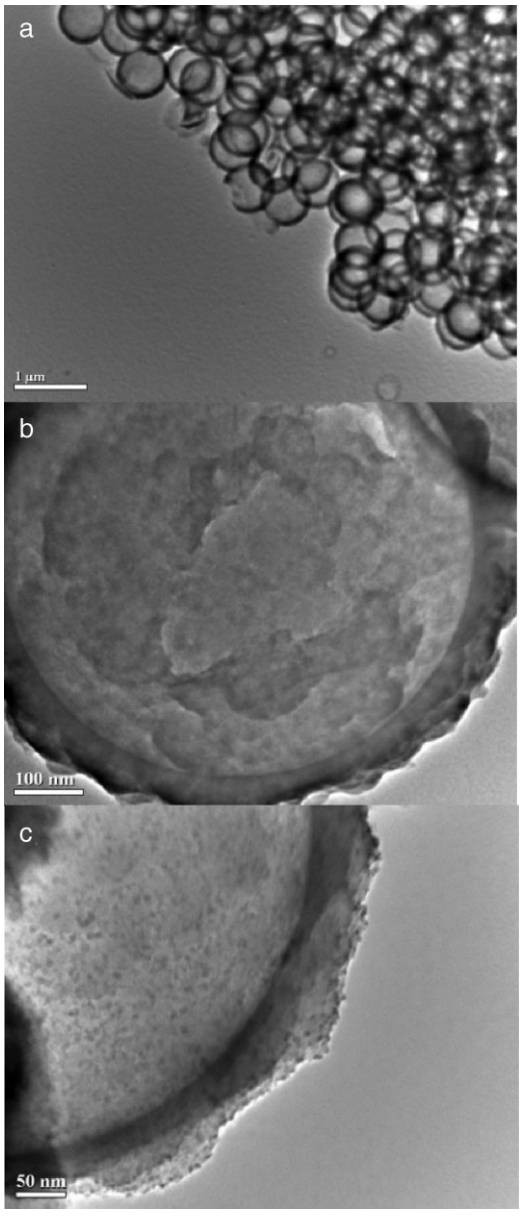


**Figure 10.** TEM images of crystalline hollow carbon spheres at a) low magnification and b) high magnification. c) TEM image of the crystalline hollow carbon spheres decorated with 1–3 nm diameter $SnO_2$ nanoparticles. Reproduced with permission from Wang et al. [221]. Copyright American Chemical Society 2006.

3DOM carbon has also been used as a basis for designing 3D-nanostructured lithium-ion batteries. Unlike other porous carbons tested, the monolithic nature of 3DOM carbon means that no binders or conducting agents are necessary when fabricating an electrode. 3DOM carbon was coated with $SnO_2$ nanoparticles in an attempt to increase the specific capacity (see Fig. 6). The charge–discharge properties of coated and uncoated 3DOM carbons were tested. The initial discharge capacity of $SnO_2$-coated carbon (278 mAh $g^{-1}$) was higher than that of


WILEY InterScience DISCOVER SOMETHING GREAT
© 2008 WILEY-VCH Verlag GmbH & Co. KGaA, Weinheim

uncoated carbon (223 mAh $g^{-1}$), but the discharge capacities were similar after the 25th cycle, showing more stable performance for the uncoated sample, probably due to detachment of $SnO_2$ particles during cycling.[21] 3DOM carbon was then used as the basis for an interpenetrating electrochemical cell. In this system, a thin, conformal polymer separator was applied to the 3DOM carbon anode. The remaining pore volume was then filled with a xerogel[174] or ambigel[175] vanadia cathode, before or after electrochemical lithiation, respectively. The xerogel system was cycled at 1 μA, showing an initial discharge capacity of 70 μAh $g^{-1}$, which decreased to 0.7 μAh $g^{-1}$ by the 100th cycle. Using an ambigel cathode, the reversible capacity of the system was greatly improved, increasing to 350 μAh $g^{-1}$, even at ten times greater current.

A graphite–glassy-carbon composite based on the 3DOM structure has also been developed.[34] A macroporous carbon monolith with mesoporous walls was first synthesized by nanocasting. In order to increase the electronic conductivity of the monolith, CVD was used to fill and/or block the mesopores with N-doped graphitic carbon. While at low rates the graphitic phase lowered the lithium capacity of the monolith compared to the as-synthesized monolith, at higher rates the graphitic phase allowed greater capacity, and helped to mitigate the formation of a solid-electrolyte interphase layer during charging.

Functionalization of a carbon surface with multilayers of nitrophenyl groups or 4-aminobenzoic acid groups has been shown to suppress the decomposition of solvent at the electrode surface without imposing a negative effect on the lithium transfer.[223,224] While these effects were demonstrated with graphite, similar functionalization of ordered porous carbons should produce the corresponding effects.

### 4.3. Capacitors/Supercapacitors

Tunable surface textures, electronic conductivity, and low density are a recurrent theme for TNCs, which makes these materials ideal candidates for electrode materials in capacitors. Current research related to porous carbon-based capacitors mainly focuses on the area of electrochemical capacitors and supercapacitors, in which charge is stored within the double layers at the interfaces between the carbon electrodes and the electrolyte. Therefore, this type of charge-storage device is also called an electrochemical double-layer capacitor (EDLC). This electrochemical design provides two advantages: 1) very high specific surface areas are easily obtained in TNCs; 2) the electric double layer is extremely thin (nm length scale) in comparison to conventional physical capacitors, in which electrodes are separated by solid dielectric materials. Since the capacitance increases with greater overlapping area and shorter distance between two electrodes, both factors contribute to the high specific capacitance of an EDLC. EDLCs are being studied extensively due to the increasing demand for new energy-storage media with high specific power and improved durability.[97] Owing to their high power densities and relatively high energy densities (compared to conventional capacitors), EDLCs are of great interest for hybrid power sources for electrical vehicles, digital telecommunications systems (e.g., cell phones, personal digital assistants (PDAs)), uninterruptible power supplies for computers, and pulse-laser generators.

For an ideal EDLC electrode material, it is necessary to have both a large surface area for charge accumulation and an interconnected porous network with sufficiently open pore windows for electrolyte wetting and rapid ionic transport. Unfortunately, currently used activated carbon electrodes from commercial products contain only micropores (<2 nm), which are not easily accessible to electrolyte ions. Moreover, even if the micropores can be wetted by the electrolyte solution, the motion of ions within these tight spaces is still restricted, limiting the achievable capacity.[97] With the above concerns, mesoporous carbon electrodes, with their more accessible porous infrastructure, are promising materials for EDLC applications.

The double-layer capacitance of TNCs correlates with the pore architecture. Activation of sol–gel-derived carbon xerogels under a gas mixture of $CO_2$ and $N_2$ increased both micro- and mesoporosity.[225] Cyclic voltammetry measurements were conducted at a fixed scan rate of 5 mV $s^{-1}$, and revealed that the capacitance increased with longer $CO_2$ activation times. Careful analysis also showed that micropores with sizes less than 0.8 nm did not contribute to the double-layer capacitance.

Through appropriate design of ordered mesoporous carbons, superior electrochemical performance over conventional microporous carbons can be achieved in EDLC applications. The mesoporous carbon SNU-1, templated from Al-MCM-48 via nanocasting,[226] exhibits regular, 3D interconnected mesopores with diameters of 2 nm.[227] In a comparison between the EDLC performance of SNU-1 and the popularly applied activated carbon MSC-25 by CV in an organic electrolyte solution, SNU-1 showed a more ideal capacitor behavior, i.e., a steeper current change at switching potentials, which resulted in a more rectangular shaped CV curve (compare with Fig. 11).[226] It was suggested that this steep change in the CV reflected the dominance of regular interconnected mesopores among the total of electrochemically

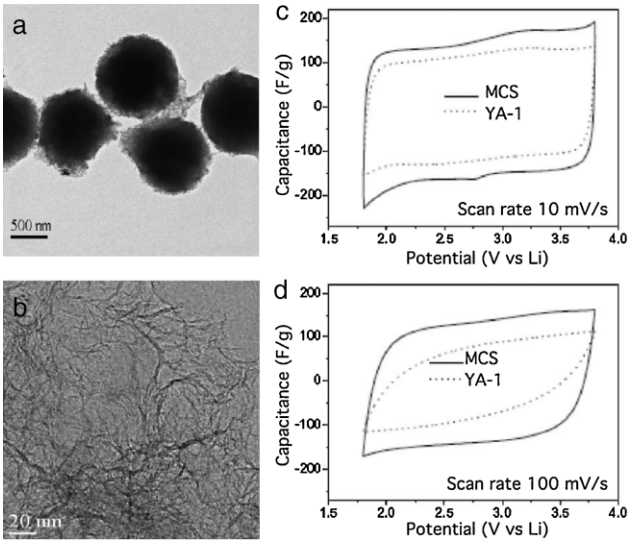


**Figure 11.** a) TEM image and b) high-resolution TEM image of nitrogen-containing mesoporous carbon spheres (MCS). Cyclic voltammetry curves of the MCS materials or the commercial activated carbon YA-1 (Calgon Mitsubishi Chemical Corporation) with different scan rates: c) 10 mV $s^{-1}$ and d) 100 mV $s^{-1}$. Reproduced with permission from Li et al. [75]. Copyright Elsevier 2007.


© 2008 WILEY-VCH Verlag GmbH & Co. KGaA, Weinheim

usable pores. When tested in an aqueous electrolyte, SNU-1 maintained a rectangular shape at scan rates as high as 20 $mV\,s^{-1}$, while MSC-25 showed a completely deformed CV curve. Unfortunately, the specific capacitance of these carbon electrodes was not reported. The EDLC performance was quite different for another mesoporous carbon, NMC, with a slightly larger mesopore size (2.3 nm) compared to that of SNU-1 (2 nm).[228] Galvanostatic charge–discharge cycling revealed that NMC (120 $F\,g^{-1}$) exhibits a much smaller specific capacitance than MSC-25 (200 $F\,g^{-1}$), probably due to a smaller surface area. However, NMC showed a higher critical scan rate and higher capacitance at faster rate than MSC-25, owing to its smaller resistance–capacitance time constant. Ordered mesoporous carbons with larger mesopores (3.3–3.9 nm), prepared via nanocasting from the mesoporous silica KIT-6, were also tested for EDLC applications.[15] Cyclic voltammetry measurements revealed that these materials have a specific capacitance up to 127 $F\,g^{-1}$, and retain more than 95% of their capacitance when the scan rate is increased from 5 to 40 $mV\,s^{-1}$.

Effects of surface functionalization on the electrochemical performance of mesoporous carbon have also been studied extensively. The surface of mesoporous carbon CMK-3 was functionalized with oxygen-containing groups by refluxing mesoporous carbons in nitric acid, and the products were tested as electrodes for EDLC.[97] The concentration of surface groups varied depending on the treatment time in nitric acid. Capacitance values were acquired from cyclic voltammograms of the mesoporous carbons in aqueous KOH electrolyte. The introduction of surface groups enhanced the capacitance via faradaic pseudocapacitance effects, and improved the high rate capacitance compared to untreated carbon. The oxidation time had to be controlled, as prolonged oxidation would cause partial collapse of the ordered channels and loss of surface area and pore volume, which is unfavorable for EDLC applications. In addition, surface oxidation impaired the conductivity of mesoporous carbons, which also slowed the charging process. The incorporation of heteroatoms also improved the electrochemical performance of mesoporous carbon electrodes. Mesoporous carbon spheres (MCS) containing nitrogen groups were synthesized via a facile polymerization-induced colloid aggregation method, using melamine–formaldehyde resin as the carbon precursor (Fig. 11).[75,229] Capacitance values as high as 150–200 $F\,g^{-1}$ were measured at high current rates. The high capacitance of the MCS was believed to arise from the presence of nitrogen groups that provided pseudocapacitance and from the high specific surface area of the material (1330–1460 $m^2\,g^{-1}$). The large and uniform mesopores (29–31 nm) also contributed to the high rate performance, by accelerating diffusion processes for ions solvated with large organic solvent molecules.

Coating of the porous carbon surface with polymers also influences the EDLC performance. Ultrathin, conformal coatings of poly(*o*-methoxyaniline) electrodeposited onto commercially available carbon aerogel substrates provided the material with faradaic pseudocapacitance.[230] However, even though the polymer film did not obstruct the interconnected mesopore/macropore network, it blocked micropores and thereby reduced the double-layer capacitance. On the other hand, extremely high capacitance values were achieved with a mesoporous carbon/polyaniline (PANI) nanocomposite prepared by in situ growth of PANI whiskers on ordered mesoporous carbon CMK-3 (see Fig. 8).[171] The capacitance of the composite was determined to be 900 $F\,g^{-1}$ at a scan rate of 0.5 $A\,g^{-1}$. Considering the amount of PANI and the capacitance contribution from pristine mesoporous carbon (150 $F\,g^{-1}$), the specific capacitance of PANI was calculated to be 1221 $F\,g^{-1}$, the highest value reported for PANI at the time. The electrode was cycled 3000 times without significant capacitance decay (less than 5%). In addition, considerable distortions were observed in both cyclic voltammetry and galvanostatic charge–discharge results, and attributed to a large pseudocapacitance.

Porous carbon-based nanocomposites synthesized by incorporating metals and metal oxides were also investigated for EDLC applications. It was reported that doping of Cu increased the capacitance of activated carbon by only a factor of 25%, probably due to the low copper loading (<1 wt %).[231] Incorporation of Ru significantly increased the capacitance. Sol–gel-derived, high surface area C-Ru xerogels exhibited a capacitance of 256 $F\,g^{-1}$ at a Ru loading of 14%.[145] The double layer accounted for 40% of this total capacitance, and the electrode could be cycled 2000 times without change. A C/Ru composite synthesized by introducing Ru into mesopores of mesoporous carbon also provided a capacitance as high as 243 $F\,g^{-1}$.[147]

### 4.4. Fuel Cells

Fuel cells are a promising alternative to current fossil-based energy-generation technologies. They produce electricity from a wide variety of energy sources or carriers, including synthesis gas, municipal wastes, hydrogen, alcohols, coal, and natural gas. More importantly, fuel cells exhibit high conversion efficiencies from fuel to electricity. Among diverse types of fuel cells, direct methanol fuel cells (DMFCs) have drawn much attention, because they can be built with small dimensions, ideal as continuous power supplies for portable electronic devices including cell phones, PDAs, and laptops. The basic unit of a DMFC is a membrane-electrode assembly, which is composed of two electrodes, one proton-exchangeable (but not electrically conductive) membrane, and one bipolar plate for current collection and feeding of methanol and air/oxygen. Auxiliary components, such as water and heat management units, are also necessary for a successful, efficient, and long-life operation of a DMFC. The core parts of DMFCs are the electrodes. These consist of a cathode for oxygen reduction, typically composed of a porous carbon support decorated with dispersed Pt nanoclusters, and an anode for methanol oxidation, composed of another porous carbon support loaded with highly dispersed Pt-Ru nanoclusters. High surface area and accessible porosity of the carbon supports are essential for the catalytic reactions during the operation of DMFCs. Commercially used catalysts are fabricated by depositing Pt onto carbon gels or activated carbon. However, due to the low accessible porosity and the dominance of micropores, Pt is only dispersed on the external surface of the carbon particles, which requires a high loading of Pt and thus increases the cost of the electrodes. Therefore, designs of novel carbon supports with large, more accessible pores are highly desired.

Both cathode and anode materials composed of porous carbon have been thoroughly investigated.[148–150,232–235] In a pioneering study, it was demonstrated that the electrochemical catalytic activity of Pt nanoclusters on ordered mesoporous carbon is


WILEY InterScience DISCOVER SOMETHING GREAT
© 2008 WILEY-VCH Verlag GmbH & Co. KGaA, Weinheim

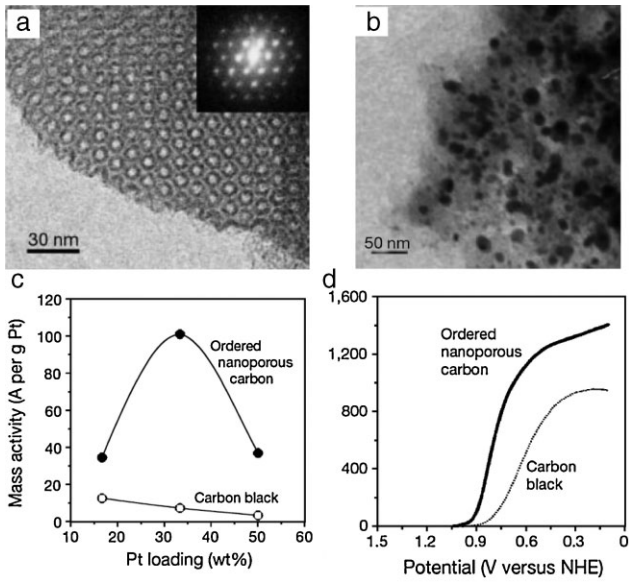


**Figure 12.** TEM images of ordered mesoporous carbon a) before and b) after loading with Pt nanoparticles. c,d) The electrochemical catalytic activity of this material was compared with conventional carbon black. Reproduced with permission from Joo et al. [148]. Copyright Nature Publishing Group 2001.

significantly improved compared to Pt supported on carbon black (Fig. 12).[148] A subsequent study evaluated both Pt and Pt-Ru nanoparticles on ordered mesoporous carbon CMK-3 substrate.[232] Gas-diffusion electrodes were prepared using these materials, and subjected to electrochemical tests. The Pt|CMK-3 cathode demonstrated better performance toward oxygen reduction than a commercial E-Tek carbon-cloth electrode, an observation which could be attributed to the size and uniformity of mesopores in CMK-3. However, the electrocatalytic activity of Pt-Ru|CMK-3 toward methanol oxidation was inferior to the commercial electrode, and the authors suggested that this could be due to a better Pt:Ru ratio and a slightly higher metal loading in the commercial materials. Another study focused on the relationship between synthesis conditions of anodes and electrochemical performance.[233] Pt-Ru nanoalloys were deposited onto porous carbon by three methods: room-temperature reduction of $H_2PtCl_6$ and $RuCl_3$ by $NaBH_4$ (PtRu-1), reduction of the two salts above using ethanol under refluxing (PtRu-2), and thermal decomposition of a single-source molecular precursor containing both Pt and Ru (PtRu-3). Electrochemical tests revealed that PtRu-3 had the highest activity toward methanol oxidation, and all three were superior to the commercial E-Tek catalyst. More interestingly, PtRu-3 also displayed the highest tolerance to carbon monoxide, which brought the possibility of using feed gas with a high CO content, thus lowering the cost for gas purification.

To lower the internal Ohmic resistance of the electrodes, it is necessary to increase the electric conductivity of porous carbon supports. One method is to introduce graphitic carbon into porous carbon via CVD, using appropriate precursors (e.g., benzene).[149,150] Electrochemical measurements revealed that Pt supported on graphitic carbons exhibited higher activity for methanol oxidation than E-Tek. Recent work by Lin et al. described the fabrication of an electrode by depositing Pt-Ru nanoparticles onto an ordered mesoporous carbon thin film with perpendicular nanochannels.[234] The electrocatalytic activity toward methanol oxidation was characterized by an anodic current, and the results were much better than for commercial products. The authors proposed that this morphology allowed easier accessibility to the Pt-Ru catalyst.

### 4.5. Hydrogen Storage

While hydrogen is widely considered a clean carrier of energy for combustion processes and fuel cells, the need for better, safe, and efficient hydrogen storage materials remains. Various forms of carbon are among the options of materials considered for hydrogen storage. In particular, nanoporous carbons merit examination for hydrogen storage applications because of their high surface areas and pore volumes, low densities, and tunable pore structures. From a comparison of different nanostructured carbons (ordered and disordered mesoporous and zeolitic carbons), it was concluded that hydrogen adsorption capacities correlate largely with the specific surface area of the material,[236] especially the surface area associated with micropores having diameters less than 0.7 nm (ultramicropores).[237] The carbon precursor greatly influences the pore texture. Hence, carbon samples prepared from sucrose exhibited higher hydrogen adsorption capacities than those synthesized from propylene or pitch, with values ranging from 1.8 wt % at 0.1 MPa to 3.5 wt % at 1 MPa at −196 °C.[237] This effect was ascribed to the larger fraction of ultramicropores in the sucrose-derived samples. Functional groups in the carbon precursor can also influence the hydrogen sorption behavior of the porous carbon product, by directing the carbon structure and texture. In a study of zeolite-templated porous carbons, nitrogen-doped products synthesized by CVD of acetonitrile exhibited higher hydrogen adsorption capacities than carbons derived by CVD of ethylene.[11] This behavior was ascribed to the tendency of nitrogen groups to hinder graphitization and maintain a larger surface area.

Treatment and functionalization of the porous carbon surface influences the hydrogen adsorption behavior both by altering the pore texture and by surface interactions with hydrogen. Carbon activation, e.g., by treatment with KOH or $CO_2$, changes the surface chemistry of carbon supports and also generates additional microporosity in the framework. This, in turn, benefits the hydrogen adsorption properties. For ordered mesoporous carbons, it was shown that the hydrogen storage capacity increased significantly after activation with either KOH[99] or $CO_2$.[100] A comparison of hydrogen sorption data for activated carbons with those of nonactivated nanostructured carbons revealed that "for a given microporous volume, the hydrogen adsorption capacity is higher for nanostructured carbon materials than for classical activated carbons."[237] This observation was tentatively related to the difference in surface chemistry between the activated and nonactivated carbons, i.e., the presence of additional acidic groups in activated carbons. If this is indeed the case, control over surface functionality should allow additional tuning of the hydrogen adsorption behavior in nanoporous carbons.

The importance of carbon surface functionality was also made clear in a study in which hydrogen was generated electro-


© 2008 WILEY-VCH Verlag GmbH & Co. KGaA, Weinheim

chemically within sucrose-derived mesoporous carbon.[207] Under ambient conditions a hydrogen storage capacity of 1.95 wt % was achieved in galvanostatic charge–discharge experiments involving water decomposition in the pores. The hydrogen-storage capacity was maintained after multiple cycles, and remained relatively high even with very fast discharge, owing to favorable transport through mesopores. During the first charging cycle, a large charge consumption was noted before the water decomposition started. In addition to a contribution by the electric double layer, significant charge uptake was attributed to reduction of oxygenated surface groups on the ordered mesoporous carbon. As in the non-electrochemical studies, a strong correlation between ultramicropore volume and the hydrogen-adsorption capacity was observed.

Overall, even the best reproducible hydrogen-uptake data obtained with nanoporous carbon materials have fallen short of the U.S. Department of Energy benchmark of 6.5 wt % at ambient temperature and pressure. Carbon samples cast from zeolite $\beta$ exhibited a particularly high hydrogen uptake of 6.9 wt % at 20 bar and 2.6 wt % at 1 bar at $-196\,^{\circ}C$.[238,239] However, for all nanoporous carbons tested, the room temperature absorption was much lower. Although the isosteric heat of adsorption in the smaller micropores (8 kJ $mol^{-1}$) is comparable to that in single-wall carbon nanotube bundles (9 kJ $mol^{-1}$) and higher than on an open graphite surface (4 kJ $mol^{-1}$), it is too small for hydrogen sorption applications at room temperature.[240] It has therefore been suggested that physisorption should be combined with chemisorption effects to enhance the hydrogen-storage behavior of carbon.[99] In this regard, further development of functionalization methods and carbon composite materials may help to pave the path to the desired target.

#### 4.6. Catalysis

Carbon materials have had a long history as commercially available support materials in heterogeneous catalysis, particularly as precious-metal catalysts for organic reactions.[200,241,242] These reactions include hydrogenation, dehydrogenation, oxidation, hydrodesulfurization, hydrodenitrogenation, hydrodeoxygenation, electrocatalytic reactions, and NO reduction. Among the desirable properties of the carbon supports are their chemical inertness, stability in the absence of molecular oxygen at high or low pH values, mechanical resistance, and high surface area. Since the introduction of ''designer carbons'', control over surface area and pore size distributions has improved significantly. Surface areas are often directly related to the dispersion of a metal catalyst. Pore size distributions are most important in catalytic reactions involving large molecules, where accessible mesopores are preferred over micropores.[241] One of the major disadvantages of traditional carbon supports,[200,241] i.e., their limited batch-to-batch reproducibility, should be, at least in part, overcome by using synthetic porous carbons. Catalyst deactivation through impurities from natural carbon is also avoidable by employing ''made-to-order'' porous carbons. Of course, variations in metal dispersion that depend on details in the catalyst preparation will still need to be controlled, even in highly ordered mesoporous carbon systems. Therefore, comparing the catalytic performance of carbon-based supports with different pore architectures remains a challenge. Typical preparations of functionalized carbon involve loading with metal precursors by ion exchange, impregnation, colloid dispersion, electroless plating, or vapor-deposition methods, followed by catalyst activation. It has been pointed out that an understanding and control of the carbon surface chemistry (surface oxygen and other heteroatoms, amphoteric character, and hydrophobicity) is as important as control over the pore structure of carbon supports.[241] The surface groups act as nucleation centers for the generation of metallic crystallites, and thereby influence the metal dispersion.[242]

A few studies have examined functionalized mesoporous carbons as heterogeneous catalysts during the last few years. When performance advantages over other carbon supports are observed, they are usually related to better catalyst dispersion and reagent/product transport through the mesoporous carbon. But activities and selectivities depend on how well the placement of catalyst particles and their size distribution can be controlled. In a comparison of Co-Mo catalysts on $\gamma$-alumina, activated carbon, and a nanoporous resorcinol–formaldehyde-based carbon as hydrodesulfurization catalysts, the overall activity of the carbon samples was greater than that of the alumina sample, because of superior metal dispersion in the higher-surface-area carbon samples.[135] But pore structure was also a determining factor. The intrinsic activity (turnover frequency) was in fact lowest in the microporous activated carbon, where metal particles blocked the pore access. Nanoporous carbon (pore sizes between 2 and 50 nm) was the winner in this comparison, largely because of the lesser diffusion limitations for reagents and because catalyst particles did not obstruct the pore openings. In contrast, a comparison of Pd-loaded ordered mesoporous carbon (Pd-CMK-3), Pd-loaded activated carbon, and Pd-loaded carbon black indicated that conversion and selectivity towards oxidation of benzylalcohol into benzaldehyde do not necessarily benefit from the ordered mesostructure.[156] Under the given conditions, conversion was highest with Pd–carbon-black, and selectivity was in fact the lowest for Pd-CMK-3. Instead of the pore architecture, the size and dispersion of Pd particles had a greater effect on the catalytic functions. It should be noted that Pd particles were located on the external surface of CMK-3, and the reactions were therefore not significantly influenced by the mesopore structure. If, on the other hand, Pd is dispersed on a molecular level within the mesopore walls, very high selectivities and conversions can be obtained. This was accomplished by coating the walls of the mesoporous silica SBA-15 with polyacrylonitrile, which provided anchoring sites for the adsorption of Pd cations, followed by carbonization of the composite and extraction of the silica.[157] The confined Pd clusters do not grow during pyrolysis, as they are stabilized by the carbon framework. In the oxidation of various alcohols to aldehydes, the selectivity of the corresponding aldehydes was greater than 99%, and a high activity was maintained over multiple runs.

An alternate method of forming metal nanoparticles within mesoporous carbon channels involves a surfactant-assisted microwave synthesis.[161] When the cationic surfactant, cetyltrimethylammonium bromide (CTAB), was added to a mixture containing ordered mesoporous carbon and a Pt precursor, the wettability of the carbon was enhanced, the Pt loading increased, and Pt nanoparticles were well dispersed throughout the mesopore system. As a result, the Pt-loaded carbon was an effective catalyst for hydrogen electro-oxidation. Pt-loaded mesoporous carbons (CMK-1 and CMK-3) employed for the


WILEY InterScience DISCOVER SOMETHING GREAT
© 2008 WILEY-VCH Verlag GmbH & Co. KGaA, Weinheim

biphasic conversion of nitrobenzene to *p*-aminophenol, required lower Pt loadings than activated carbon supports, and displayed greater selectivity.[243] The difference in performance was attributed to the higher catalyst dispersion on the mesoporous supports and the lower pore diffusion resistance in these structured materials. It should be noted that good metal dispersion does not always lead to the expected performance advantages, as seen when a mesoporous carbon xerogel prepared from resorcinol–formaldehyde precursors was activated in oxygen, impregnated with a Pd salt, reduced using sodium formate or hydrogen, and then tested as a catalyst for enantioselective hydrogenation of isophorone and of (*E*)-2-benzylidene-1-benzosuberone.[244] Pd particle size and dispersion were strongly influenced by the choice of reducing agent. In this study, the catalyst with smaller metal dispersion afforded a higher enantiomeric excess.

Reagent transport is even easier in 3DOM carbons with interconnected pores that have diameters exceeding 100 nm. When 3DOM carbon with graphitic walls was coated with Pt nanoparticles and examined as a catalyst for the electrochemical oxidation of methanol, its activity was greater than that of a commercial Pt-carbon black reference sample, even though the well-dispersed Pt nanoparticles were larger than in the commercial sample.[154] This was attributed to the good access of reactants and products to the interconnected pore structure in the 3DOM sample, and to the higher graphitic content and the associated higher electrical conductivity in that sample.

In addition to being an efficient metal-catalyst support, synthetic carbon is a useful support for acid catalysis. In a recent study, the hexagonally ordered mesoporous carbon CMK-5 was functionalized with sulfonic acid groups by covalent attachment of sulfonic-acid-containing aryl radicals, and examined as an acid catalyst for the formation of bisphenol-A and for esterification of acetic acid with ethanol.[104] Compared to sulfonic-acid-functionalized mesoporous silica supports, the carbon sample was more stable towards surface-group detachment and degradation by hydrolysis. It also exhibited higher turnover numbers. The superior catalytic performance was ascribed in part to the hydrophobic nature of the support, which may synergistically influence the catalytic activity of the hydrophilic surface groups. Mesoporous carbons derived by low-temperature (400 °C) carbonization of starch provide an alternate backbone for sulfonation.[103] After treatment of these so-called Starbon® materials with sulfuric acid, the products become highly active catalysts for esterification of diacids, liquid-phase acylation of alcohols, and alkylation of aromatic substrates.

Sulfonic acid groups can also be introduced directly during a carbon synthesis, by incomplete carbonization of sulfonated aromatic compounds, such as naphthalene. Even though the product obtained in a study using this approach was amorphous and had a relatively low surface area, it presented a high density of sulfonic acid groups, and rivaled the performance of sulfuric acid as a catalyst for esterification of acetic acid.[245] However, when this soft material was tested for esterification of higher fatty acids for biodiesel production, the aromatic molecules leached out. Such leaching could be avoided by starting with glucose and sucrose molecules instead, carbonizing these incompletely at low temperature, and treating them with sulfuric acid.[246] The product could be molded into hard pellets or thin flexible films. Its activity in the esterification of oleic acid and stearic acid (both vegetable-oil constituents) was stated to be more than half that of liquid sulfuric acid, and higher than that of conventional solid acid catalysts. One might anticipate that the addition of uniform mesopores to such a material could bring additional performance advantages.

Beyond acting as supports for metal and acid catalysis, porous carbons lend themselves as host structures for biocatalysts, such as enzymes. To prevent leaching of the enzyme during a reaction, it can be crosslinked within the pore structure, a procedure that led to an effective bio-electrocatalyst based on glucose oxidase supported in mesocellular carbon foam.[247]

### 4.7. Sorption

Carbonaceous materials are common sorbents in both gas–solid and liquid–solid environments. Functionalized glassy carbon and porous graphitic-carbon particles have also been investigated as stationary phases for chromatography, including electrochemically modulated liquid chromatography (EMLC).[248] Naturally, nonfunctionalized and functionalized ordered mesoporous carbons are also being considered for sorption applications. For example, a mesoporous carbon impregnated with ferrous chloride and oxidized with sodium hypochlorite was used as a sorbent for removing arsenic from drinking water.[140] Perhaps the greatest attraction of mesoporous and macroporous carbons with designed porosity is their ability to accommodate relatively large guests, such as enzymes and other biomolecules. Adsorption of enzymes on porous carbon is of interest for potential applications in biosensing, enzymatic catalysis, biotechnology, medical technology, and food processing. Mesoporous carbons, in particular, provide an opportunity for selective adsorption of proteins and other biomolecules with specific molecular sizes, because their textural parameters are readily tunable.[249,250] Without a surface charge, porous carbon interferes less with the structure and orientation of active centers in enzymes than, for example, porous silicas, where surface silanol groups interact electrostatically with amino acid residues.[250] In studies of enzyme immobilization on carbon, it was demonstrated that the antimicrobial enzyme lysozyme can adsorb within the channels of a carbon molecular sieve without denaturing.[1,250] The enzyme loading depends on the pore structure and the solution pH. The maximum adsorption occurred at a pH close to the isoelectric point of lysozyme, when electrostatic repulsion between enzyme molecules was minimal, so that the molecules could pack more tightly. The relatively high corresponding pH (pH = 11) would have resulted in deterioration of a silica-based mesoporous sieve, but the structural integrity of the carbon sieve was preserved. A further increase in adsorption capacity was achieved by functionalizing the mesoporous carbon surface with carboxyl groups using ammonium persulfate as an oxidizing agent.[95] This oxidation process not only changed the wettability and surface interactions of the porous carbon, but also modified the pore structure, thereby facilitating access of the protein to adsorption sites. Other biomolecules whose adsorption on ordered mesoporous carbons has been studied include cytochrome C, histidine, catechin, vitamin E, and the endocrine disrupter nonylphenol.[249,251,252] As this area progresses, it can benefit from prior


© 2008 WILEY-VCH Verlag GmbH & Co. KGaA, Weinheim

experience with nonporous carbon systems. Surface modification techniques that have been used to anchor polypeptides to graphitic carbon should also be suitable for synthetic porous carbons. As one example, poly(L-cysteine) functionalization was achieved on graphite powder by initial derivatization with 4-nitrophenyl moieties, reduction of the nitro groupsm and coupling to poly(S-benzyl-L-cysteine) via an amide linkage.[116] After deprotection of the thiol groups, the resulting functionalized carbon was able to quantitatively complex cadmium(II) ions. Because grafting of 4-nitrophenyl moieties has been accomplished on ordered porous carbons, similar step-by-step modification processes should be possible in the confinement of large mesopores and macropores.

### 4.8. Magnetic Materials

Various applications of porous carbons, including those involving encapsulation, require recycling or separation of the carbon from the rest of the system after the carbon has carried out its desired function. As an alternative to filtration or centrifugation, a convenient method of isolating carbonaceous solids is by rendering them magnetic and attracting them to external magnetic fields. Several studies have shown that incorporation of magnetic nanoparticles in porous carbons makes this possible. To maintain the advantages of the porous support, it is important to avoid pore blockage and magnetic-particle aggregation when the magnetic components are added. These components should also not interfere with other functionalities in the system, nor leach out during use. One elegant way of satisfying these criteria involves selective deposition of surface-protected cobalt nanoparticles on the external surface of an ordered mesoporous carbon.[253] First, cobalt nanoparticles were grafted onto a nanocast, mesostructured carbon–silica SBA-15 composite material. They were coated by a nanometer-thick carbon layer, to protect them against subsequent corrosion and to prevent sintering. The silica mold was then removed by extraction with hydrofluoric acid. At this stage, mesopores were accessible for sorption of dye molecules or for loading with Pd catalyst particles for hydrogenation of octene. Separation of the material from the solution with a magnet was straightforward (Fig. 13). A somewhat simpler method entails incorporation of iron species in the carbon precursor used for nanocasting in a mesoporous silica template.[164] After the resulting polypyrrole/$Fe^{2+}$/SBA-15 nanocomposite was carbonized, and silica was removed by boiling in NaOH solution, supermagnetic $\alpha$-Fe and $Fe_3C$ nanoparticles were embedded in the carbon walls, leaving mesopores open for other guest species. In this procedure, it was critical to allow long polymerization times to obtain ordered mesostructures and slow heating rates to avoid formation of large (>50 nm) ferromagnetic particles outside the mesoporous carbon particles. It should be noted that the iron precursor initially acts as a Lewis acid to catalyze the polymerization process. Cobalt and nickel salts can also function as polymerization catalysts (e.g., for poly(furfuryl alcohol)), and subsequently be reduced to magnetic nanoparticles during carbonization.[163]

A similar nanocasting procedure was used to prepare mesoporous carbon foam with well-dispersed $\alpha$-Fe and $Fe_3O_4$ nanoparticles.[247] After the pores of the magnetic composite were loaded with the enzyme glucose oxidase, the material could be employed as a magnetically switchable bio-electrocatalytic system. During cyclic-voltammetric experiments, the current produced by the enzyme-catalyzed oxidation of glucose was controlled by magnetically positioning the composite particles near or away from the electrode surface. Crosslinking of the enzyme with glutaraldehyde prevented it from leaching out of the porous host. In another study, ordered mesoporous carbon decorated with nickel nanoparticles was examined as a magnetically separable adsorbent for vitamin B2.[159]

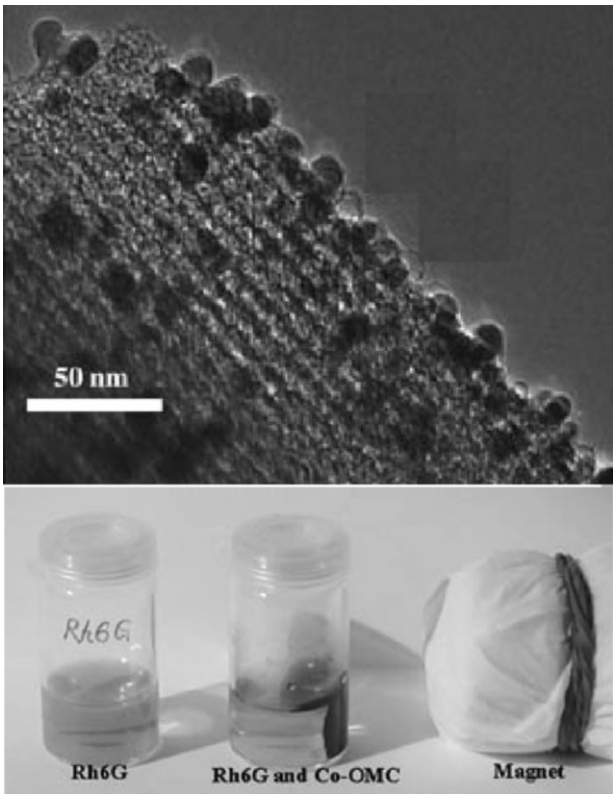


**Figure 13.** Top: TEM image of a cobalt-decorated ordered mesoporous carbon (Co-OMC). Bottom: An aqueous solution of the dye Rh6G before and after adsorption on Co-OMC and separation of the solid particles by a magnet. Reproduced with permission from Lu et al. [253].

It is notable that when metallic nanoparticles are incorporated within mesoporous or graphene-like carbon shells, they are protected against attack by concentrated acids or bases[155,163,254] and against oxidation.[255] Entrapment of catalytic metal nanoparticles within a mesoporous carbon shell may protect the catalyst and prevent its aggregation when such a hollow core/shell structure is used as a size-selective microreactor system.[256]

## 5. Conclusions and Outlook

While tremendous progress has been made in syntheses of porous carbons with new morphologies, exciting opportunities remain for functionalizing such materials to optimize their properties for specific applications. Addition of surface groups


WILEY InterScience DISCOVER SOMETHING GREAT

© 2008 WILEY-VCH Verlag GmbH & Co. KGaA, Weinheim

permits modification of pore texture, pore wettability, and surface reactivity.

For textural modification, polymer[175] or polyelectrolyte[98] coatings can be used to block micropores and reduce surface areas of the support if desired. Surface oxidation achieves the opposite effect, an increase in microporosity and specific surface area, as long as the overall skeletal structure remains largely intact. Molecular groups grafted to mesopore surfaces can be used to fine-tune free pore diameters, and thereby control molecular transport through the pores. The next step could be dynamic control of pore access via external activators (such as pH), a feature that has already been incorporated in some silica-based porous materials.[257]

Pore wettability, surface hydrophobicity, and hydrophilicity all depend on the type of functional group present, and determine penetration of reactants into the pore system. As-synthesized carbon materials produced by high-temperature carbonization are hydrophobic, and therefore suitable for uptake of components in oil, aromatic substances, and other nonpolar systems. Super-hydrophobic properties can be achieved through fluorination. Surface oxidation, sulfonation, or introduction of other charged groups renders the pore surfaces more accessible to polar fluids. Addition of polyelectrolytes to the surface can be used to increase surface charges further, and to provide electrostatic attachment points. Surface polarity is a critical consideration, not only for host–guest applications, but also influences the propensity of the material for further functionalization.

In terms of surface reactivity, the ability to establish carboxylate groups, para-functionalized benzene groups, and reactive double bonds on the porous carbon surface provides anchoring points for endless other organic groups. Currently, electrochemical functionalization seems to be the optimum method. Not only does it produce C–C bonds that are more stable to hydrolysis and desorption than carboxylate-based linkages, but electrochemically driven modifications often proceed considerably faster than other heterogeneous processes, which merely involve stirring of the carbonaceous material in a reactant solution.

With respect to applications, designed porous carbons promise tremendous benefits over traditional carbon systems, particularly for high-value applications. In large volume applications, such as treatment of waste waters, it is still difficult to compete with lower-cost activated carbons. More advanced applications, related to the energy field, sensing, and fine chemical reactions, on the other hand, are likely to reap significant benefits from the tunability of functionalized ordered porous carbon structures. For catalysis, the new carbon systems provide ways to improve the selectivity of a catalyst, enhance metal dispersion or coverage of other active groups, and increase the overall activity of the catalyst. In synthesis applications, the hydrothermal stability of ordered porous carbons permits these materials to be applied as nanoreactors, to produce very uniform nanoparticles or other products.[258,259] Functionalization of the nanoreactor surface is likely to influence the product properties. For carbon-based sensors, better selectivity and specific detection of one or perhaps several distinct molecules will be achievable by functionalizing porous carbon electrodes. Besides the applications mentioned in this review, other applications that may benefit from the field include reactive inks, thermal and sound insulation, camouflage and stealth operations, solar and thermophotovoltaic harnessing of energy, and probably more.

So, what is next? The number of functionalization methods that have been applied to porous designer carbons is rising, but still open for significant growth, aided by the field of synthetic organic chemistry. Better control over the density, stability and specific location of surface functional groups would be desirable. In mesoporous silicates, incorporation of multiple functional groups has been found advantageous for some systems,[260] and similar approaches can be used for porous carbons. In carbon materials with hierarchical pore structure, it would be particularly interesting to locate one type of functionality in pores of one size (e.g., mesopores), a different functionality in pores of another size (e.g., macropores), and yet another functionality on the external particle surface. The concept of site-specific functionalization is achievable, and has already been illustrated, for example, for magnetic carbon-supported catalysts, but the system complexity can likely be increased in the future.[253] Another demonstration of the elaborate structure achievable around functionalized ordered porous carbons is given by the 3D interpenetrating lithium-ion cell described earlier, in which 3DOM carbon is coated by an ultrathin polymer separation layer, and infiltrated with a sol–gel-based cathode material.[175] Here, too, the degree of sophistication can be increased further, perhaps by combining battery functionality with supercapacitor properties in one carbon-based system, or by blending hydrogen storage with fuel cell functions in one integrated system.

In the future, we may also see further incorporation of designed porous carbons into biosystems. Functionalization methods will enhance the compatibility of carbon with other materials, both hard and soft, to allow immobilization of proteins, DNA, and enzymes, or to facilitate in vivo drug delivery. As mentioned earlier, proof for these concepts has already been given, but the spectrum of applications is bound to broaden.

Carbon has a history of revolutionizing our world. By learning how to modify and structure carbon on a small scale, we might end up improving this world in a big way.

## Acknowledgements

The authors acknowledge financial support from the National Science Foundation (DMR-0704312 and CBET-0730437), the Office of Naval Research (Grant N00014-07-1-0608) and the Petroleum Research Foundation administered by the American Chemical Society (Grant 42751-AC10).

Received: May 31, 2008
Revised: July 15, 2008
Published online:

[1] A. Vinu, M. Miyahara, K. Ariga, *J. Phys. Chem. B* **2005**, *109*, 6436.
[2] M. T. Gilbert, J. H. Knox, B. Kaur, *Chromatographia* **1982**, *16*, 138.
[3] R. Ryoo, S. H. Joo, S. Jun, *J. Phys. Chem. B* **1999**, *103*, 7743.
[4] S. Jun, S. H. Joo, R. Ryoo, M. Kruk, M. Jaroniec, Z. Liu, T. Ohsuna, O. Terasaki, *J. Am. Chem. Soc.* **2000**, *122*, 10712.
[5] M. Kruk, M. Jaroniec, R. Ryoo, S. H. Joo, *J. Phys. Chem. B* **2000**, *104*, 7960.
[6] F. Su, L. Lv, X. S. Zhao, *Int. J. Nanosci.* **2005**, *4*, 261.


© 2008 WILEY-VCH Verlag GmbH & Co. KGaA, Weinheim

[7] H. Li, Y. Sakamoto, Y. Li, O. Terasaki, M. Thommes, S. Che, *Microporous Mesoporous Mater.* **2006**, *95*, 193.
[8] J. Lee, K. Sohn, T. Hyeon, *Chem. Commun.* **2002**, 2674.
[9] A.-H. Lu, W.-C. Li, W. Schmidt, F. Schueth, *Microporous Mesoporous Mater.* **2005**, *80*, 117.
[10] X. Wang, K. N. Bozhilov, P. Feng, *Chem. Mater.* **2006**, *18*, 6373.
[11] Z. Yang, Y. Xia, X. Sun, R. Mokaya, *J. Phys. Chem. B* **2006**, *110*, 18424.
[12] A. A. Zakhidov, R. H. Baughman, Z. Iqbal, C. Cui, I. Khayrullin, O. Dantas, J. Marti, V. G. Ralchenko, *Science* **1998**, *282*, 897.
[13] J. Lee, K. Sohn, T. Hyeon, *J. Am. Chem. Soc.* **2001**, *123*, 5146.
[14] Y. Meng, D. Gu, F. Zhang, Y. Shi, H. Yang, Z. Li, C. Yu, B. Tu, D. Zhao, *Angew. Chem. Int. Ed.* **2005**, *44*, 7053.
[15] L. Zhou, H. Li, C. Yu, X. Zhou, J. Tang, Y. Meng, Y. Xia, D. Zhao, *Carbon* **2006**, *44*, 1601.
[16] H. Kosonen, S. Valkama, A. Nykanen, M. Toivanen, G. ten Brinke, J. Ruokolainen, O. Ikkala, *Adv. Mater.* **2006**, *18*, 201.
[17] C. Lin, J. A. Ritter, *Carbon* **1997**, *35*, 1271.
[18] K. T. Lee, S. M. Oh, *Chem. Commun.* **2002**, 2722.
[19] E. J. Zanto, S. A. Al-Muhtaseb, J. A. Ritter, *Ind. Eng. Chem. Res.* **2002**, *41*, 3151.
[20] S. A. Al-Muhtaseb, J. A. Ritter, *Adv. Mater.* **2003**, *15*, 101.
[21] K. T. Lee, J. C. Lytle, N. S. Ergang, S. M. Oh, A. Stein, *Adv. Funct. Mater.* **2005**, *15*, 547.
[22] Y. Xia, R. Mokaya, *Chem. Mater.* **2005**, *17*, 1553.
[23] C.-M. Yang, C. Weidenthaler, B. Spliethoff, M. Mayanna, F. Schueth, *Chem. Mater.* **2005**, *17*, 355.
[24] T.-W. Kim, I.-S. Park, R. Ryoo, *Angew. Chem. Int. Ed.* **2003**, *42*, 4375.
[25] H. Yang, Y. Yan, Y. Liu, F. Zhang, R. Zhang, Y. Meng, M. Li, S. Xie, B. Tu, D. Zhao, *J. Phys. Chem. B* **2004**, *108*, 17320.
[26] K. P. Gierszal, T.-W. Kim, R. Ryoo, M. Jaroniec, *J. Phys. Chem. B* **2005**, *109*, 23263.
[27] C. H. Kim, D.-K. Lee, T. J. Pinnavaia, *Langmuir* **2004**, *20*, 5157.
[28] Y. Xia, R. Mokaya, *Adv. Mater.* **2004**, *16*, 886.
[29] C. Liang, Z. Li, S. Dai, *Angew. Chem. Int. Ed.* **2008**, *47*, 3696.
[30] A. Sayari, Y. Yang, *Chem. Mater.* **2005**, *17*, 6108.
[31] Y. Xia, Z. Yang, R. Mokaya, *Stud. Surf. Sci. Catal.* **2005**, *156*, 565.
[32] Z. Wang, F. Li, A. Stein, *Nano Lett.* **2007**, *7*, 3223.
[33] M. Steinhart, C. Liang, G. W. Lynn, U. Goesele, S. Dai, *Chem. Mater.* **2007**, *19*, 2383.
[34] Z. Wang, F. Li, N. S. Ergang, A. Stein, *Chem. Mater.* **2006**, *18*, 5543.
[35] Z. Wang, A. Stein, *Chem. Mater.* **2008**, *20*, 1029.
[36] R. Ryoo, S. H. Joo, M. Kruk, M. Jaroniec, *Adv. Mater.* **2001**, *13*, 677.
[37] H. Yang, D. Zhao, *J. Mater. Chem.* **2005**, *15*, 1217.
[38] Z. Li, M. Jaroniec, *J. Am. Chem. Soc.* **2001**, *123*, 9208.
[39] Z. Li, M. Jaroniec, *J. Phys. Chem. B* **2004**, *108*, 824.
[40] K. P. Gierszal, M. Jaroniec, *J. Am. Chem. Soc.* **2006**, *128*, 10026.
[41] W. M. Qiao, Y. Song, S. H. Hong, S. Y. Lim, S. H. Yoon, Y. Korai, I. Mochida, *Langmuir* **2006**, *22*, 3791.
[42] S. B. Yoon, K. Sohn, J. Y. Kim, C.-H. Shin, J.-S. Yu, T. Hyeon, *Adv. Mater.* **2002**, *14*, 19.
[43] M. Kim, S. B. Yoon, K. Sohn, J. Y. Kim, C.-H. Shin, T. Hyeon, J.-S. Yu, *Microporous Mesoporous Mater.* **2003**, *63*, 1.
[44] D. Kawashima, T. Aihara, Y. Kobayashi, T. Kyotani, A. Tomita, *Chem. Mater.* **2000**, *12*, 3397.
[45] C. Liang, K. Hong, G. A. Guiochon, J. W. Mays, S. Dai, *Angew. Chem. Int. Ed.* **2004**, *43*, 5785.
[46] Z. Li, W. Yan, S. Dai, *Carbon* **2004**, *42*, 767.
[47] F. Zhang, Y. Meng, D. Gu, Y. Yan, C. Yu, B. Tu, D. Zhao, *J. Am. Chem. Soc.* **2005**, *127*, 13508.
[48] C. Liang, S. Dai, *J. Am. Chem. Soc.* **2006**, *128*, 5316.
[49] Y. Meng, D. Gu, F. Zhang, Y. Shi, L. Cheng, D. Feng, Z. Wu, Z. Chen, Y. Wan, A. Stein, D. Zhao, *Chem. Mater.* **2006**, *18*, 4447.
[50] F. Zhang, Y. Meng, D. Gu, Y. Yan, Z. Chen, B. Tu, D. Zhao, *Chem. Mater.* **2006**, *18*, 5279.
[51] R. Liu, Y. Shi, Y. Wan, Y. Meng, F. Zhang, D. Gu, Z. Chen, B. Tu, D. Zhao, *J. Am. Chem. Soc.* **2006**, *128*, 11652.
[52] F. Zhang, D. Gu, T. Yu, F. Zhang, S. Xie, L. Zhang, Y. Deng, Y. Wan, B. Tu, D. Zhao, *J. Am. Chem. Soc.* **2007**, *129*, 7746.
[53] Y. Huang, H. Cai, T. Yu, F. Zhang, F. Zhang, Y. Meng, G. Dong, Y. Wan, X. Sun, B. Tu, D. Zhao, *Angew. Chem. Int. Ed.* **2007**, *46*, 1089.
[54] Y. Deng, T. Yu, Y. Wan, S. Shi, Y. Meng, D. Gu, L. Zhang, Y. Huang, C. Liu, X. Wu, D. Zhao, *J. Am. Chem. Soc.* **2007**, *129*, 1690.
[55] Y. Huang, H. Cai, T. Yu, X. Sun, B. Tu, D. Zhao, *Chem. Asian J.* **2007**, *2*, 1282.
[56] Y. Deng, C. Liu, D. Gu, T. Yu, B. Tu, D. Zhao, *J. Mater. Chem.* **2008**, *18*, 91.
[57] Y. Wan, X. Qian, N. Jia, Z. Wang, H. Li, D. Zhao, *Chem. Mater.* **2008**, *20*, 1012.
[58] A.-H. Lu, W. Schmidt, B. Spliethoff, F. Schueth, *Adv. Mater.* **2003**, *15*, 1602.
[59] J. Lee, J. Kim, T. Hyeon, *Chem. Commun.* **2003**, 1138.
[60] A.-H. Lu, W.-C. Li, W. Schmidt, F. Schueth, *Microporous Mesoporous Mater.* **2006**, *95*, 187.
[61] B.-L. Su, A. Vantomme, L. Surahy, R. Pirard, J.-P. Pirard, *Chem. Mater.* **2007**, *19*, 3325.
[62] Y. Deng, C. Liu, T. Yu, F. Liu, F. Zhang, Y. Wan, L. Zhang, C. Wang, B. Tu, P. A. Webley, H. Wang, D. Zhao, *Chem. Mater.* **2007**, *19*, 3271.
[63] Z. Wang, E. R. Kiesel, A. Stein, *J. Mater. Chem.* **2008**, *18*, 2194.
[64] J. Lee, J. Kim, T. Hyeon, *Adv. Mater.* **2006**, *18*, **2073**.
[65] A.-H. Lu, F. Schueth, *Adv. Mater.* **2006**, *18*, 1793.
[66] Y. Wan, Y. Shi, D. Zhao, *Chem. Mater.* **2008**, *20*, 932.
[67] F. Su, Z. Zhou, W. Guo, J. Liu, X. N. Tian, X. S. Zhao, *Chem. Phys. Carbon* **2008**, *30*, 63.
[68] A. Stein, B. J. Melde, R. C. Schroden, *Adv. Mater.* **2000**, *12*, 1403.
[69] N. Tsubokawa, *Bull. Chem. Soc. Jpn.* **2002**, *75*, 2115.
[70] N. Tsubokawa, *Polym. J.* **2005**, *37*, 637.
[71] P. Liu, *Eur. Polym. J.* **2005**, *41*, 2693.
[72] S. Banerjee, T. Hemraj-Benny, S. S. Wong, *Adv. Mater.* **2005**, *17*, 17.
[73] A. Lu, A. Kiefer, W. Schmidt, F. Schueth, *Chem. Mater.* **2004**, *16*, 100.
[74] Y. Shin, G. E. Fryxell, W. Um, K. Parker, S. V. Mattigod, R. Skaggs, *Adv. Funct. Mater.* **2007**, *17*, 2897.
[75] W. Li, D. Chen, Z. Li, Y. Shi, Y. Wan, G. Wang, Z. Jiang, D. Zhao, *Carbon* **2007**, *45*, 1757.
[76] A. Vinu, P. Shrinivasu, D. P. Sawant, T. Mori, K. Ariga, J. S. Chang, S. H. Jhung, V. V. Balasubramanian, Y. K. Hwang, *Chem. Mater.* **2007**, *19*, 4397.
[77] Y. Shin, G. E. Fryxell, C. A. Johnson, II, M. M. Haley, *Chem. Mater.* **2008**, *20*, 981.
[78] A. Vinu, K. Ariga, T. Mori, T. Nakanishi, S. Hishita, D. Golberg, Y. Bando, *Adv. Mater.* **2005**, *17*, 1648.
[79] A. Vinu, M. Terrones, D. Golberg, S. Hishita, K. Ariga, T. Mori, *Chem. Mater.* **2005**, *17*, 5887.
[80] A. Vinu, *Adv. Funct. Mater.* **2008**, *18*, 816.
[81] M.-M. Titirici, A. Thomas, M. Antonietti, *J. Mater. Chem.* **2007**, *17*, 3412.
[82] Y. Xia, R. Mokaya, *Adv. Mater.* **2004**, *16*, 1553.
[83] Y. Xia, R. Mokaya, *J. Phys. Chem. C* **2007**, *111*, 10035.
[84] S. Tanaka, N. Nishiyama, Y. Egashira, K. Ueyama, *Chem. Commun.* **2005**, 2125.
[85] T. Yu, Y. Deng, L. Wang, R. Liu, L. Zhang, B. Tu, D. Zhao, *Adv. Mater.* **2007**, *19*, 2301.
[86] R. Liu, Y. Ren, Y. Shi, F. Zhang, L. Zhang, B. Tu, D. Zhao, *Chem. Mater.* **2008**, *20*, 1140.
[87] P. E. Fanning, M. A. Vannice, *Carbon* **1993**, *31*, 721.
[88] P.-Z. Cheng, H. Teng, *Carbon* **2003**, *41*, **2057**.
[89] J. Zawadzki, *Chem. Phys. Carbon* **1989**, *21*, 147.
[90] Y. Otake, R. G. Jenkins, *Carbon* **1993**, *31*, 109.
[91] P. Vinke, M. van der Eijk, M. Verbree, A. F. Voskamp, H. van Bekkum, *Carbon* **1994**, *32*, 675.
[92] B. K. Pradhan, N. K. Sandle, *Carbon* **1999**, *37*, 1323.


© 2008 WILEY-VCH Verlag GmbH & Co. KGaA, Weinheim

[93] X. Chen, M. Farber, Y. Gao, I. Kulaots, E. M. Suuberg, R. H. Hurt, *Carbon* **2003**, *41*, 1489.
[94] P. A. Bazula, A.-H. Lu, J.-J. Nitz, F. Schueth, *Microporous Mesoporous Mater.* **2008**, *108*, 266.
[95] A. Vinu, K. Z. Hossian, P. Srinivasu, M. Miyahara, S. Anandan, N. Gokulakrishnan, T. Mori, K. Ariga, V. V. Balasubramanian, *J. Mater. Chem.* **2007**, *17*, 1819.
[96] A.-H. Lu, W.-C. Li, N. Muratova, B. Spliethoff, F. Schueth, *Chem. Commun.* **2005**, 5184.
[97] H. Li, H. A. Xi, S. Zhu, Z. Wen, R. Wang, *Microporous Mesoporous Mater.* **2006**, *96*, 357.
[98] Z. Wang, N. S. Ergang, M. A. Al-Daous, A. Stein, *Chem. Mater.* **2005**, *17*, 6805.
[99] M. Choi, R. Ryoo, *J. Mater. Chem.* **2007**, *17*, 4204.
[100] K. Xia, Q. Gao, C. Wu, S. Song, M. Ruan, *Carbon* **2007**, *45*, 1989.
[101] Y. Yan, J. Wei, F. Q. Zhang, Y. Meng, B. Tu, D. Y. Zhao, *Microporous Mesoporous Mater.* **2008**, *113*, 305.
[102] J. Gorka, A. Zawislak, J. Choma, M. Jaroniec, *Carbon*, **2008**, *46*, 1159.
[103] V. L. Budarin, J. H. Clark, R. Luque, D. J. Macquarrie, *Chem. Commun.* **2007**, 634.
[104] X. Wang, R. Liu, M. M. Waje, Z. Chen, Y. Yan, K. N. Bozhilov, P. Feng, *Chem. Mater.* **2007**, *19*, 2395.
[105] R. Xing, Y. Liu, Y. Wang, L. Chen, H. Wu, Y. Jiang, M. He, P. Wu, *Microporous Mesoporous Mater.* **2007**, *105*, 41.
[106] Z. Li, G. D. Del Cul, W. Yan, C. Liang, S. Dai, *J. Am. Chem. Soc.* **2004**, *126*, 12782.
[107] L. Wang, Y. Zhao, K. Lin, X. Zhao, Z. Shan, Y. Di, Z. Sun, X. Cao, Y. Zou, D. Jiang, L. Jiang, F.-S. Xiao, *Carbon* **2006**, *44*, 1336.
[108] S. M. Mukhopadhyay, R. V. Pulikollu, A. K. Roy, *Appl. Surf. Sci.* **2004**, *225*, 223.
[109] H. P. Boehm, *Carbon* **1994**, *32*, 759.
[110] S. Jun, M. Choi, S. Ryu, H.-Y. Lee, R. Ryoo, *Stud. Surf. Sci. Catal.* **2003**, *146*, 37.
[111] D. Yu, Z. Wang, N. S. Ergang, A. Stein, *Stud. Surf. Sci. Catal.* **2007**, *165*, 365.
[112] M. Delamar, R. Hitmi, J. Pinson, J. M. Saveant, *J. Am. Chem. Soc.* **1992**, *114*, 5883.
[113] Z. Li, W. Yan, S. Dai, *Langmuir* **2005**, *21*, 11999.
[114] Z. Li, S. Dai, *Chem. Mater.* **2005**, *17*, 1717.
[115] M. Pandurangappa, N. S. Lawrence, R. G. Compton, *Analyst* **2002**, *127*, 1568.
[116] G. G. Wildgoose, H. C. Leventis, I. J. Davies, A. Crossley, N. S. Lawrence, L. Jiang, T. G. J. Jones, R. G. Compton, *J. Mater. Chem.* **2005**, *15*, 2375.
[117] C. Liang, J.-F. Huang, Z. Li, H. Luo, S. Dai, *Eur. J. Org. Chem.* **2006**, 586.
[118] X. Wang, D.-E. Jiang, S. Dai, *Chem. Mater.* **2008**, *20*, 4800.
[119] K. H. Vase, A. H. Holm, K. Norrman, S. U. Pedersen, K. Daasbjerg, *Langmuir* **2007**, *23*, 3786.
[120] L. Bi, J. Liu, Y. Shen, J. Jiang, S. Dong, *New J. Chem.* **2003**, *27*, 756.
[121] M. Abe, K. Kawashima, K. Kozawa, H. Sakai, K. Kaneko, *Langmuir* **2000**, *16*, 5059.
[122] H. Tamai, K. Shiraki, T. Shiono, H. Yasuda, *J. Colloid Interface Sci.* **2006**, *295*, 299.
[123] C. U. Pittman, Jr, Z. Wu, W. Jiang, G. R. He, B. Wu, W. Li, S. D. Gardner, *Carbon* **1997**, *35*, 929.
[124] J. Economy, K. Foster, A. Andreopoulos, H. Jung, *Chem. Tech.* **1992**, *22*, 597.
[125] C. L. Mangun, K. R. Benak, J. Economy, K. L. Foster, *Carbon* **2001**, *39*, 1809.
[126] V. L. Budarin, J. H. Clark, S. J. Tavener, K. Wilson, *Chem. Commun.* **2004**, 2736.
[127] M. Toupin, D. Belanger, *J. Phys. Chem. C* **2007**, *111*, 5394.
[128] F. Cosnier, A. Celzard, G. Furdin, D. Begin, J. F. Mareche, O. Barres, *Carbon* **2005**, *43*, 2554.
[129] B. Fang, L. Binder, *J. Phys. Chem. B* **2006**, *110*, 7877.
[130] S. Ching, R. C. Dudek, E. A. Tabet, W. S. Willis, S. L. Suib, *Langmuir* **1994**, *10*, 1657.
[131] B. Sun, P. E. Colavita, H. Kim, M. Lockett, M. S. Marcus, L. M. Smith, R. J. Hamers, *Langmuir* **2006**, *22*, 9598.
[132] R. J. Chen, Y. Zhang, D. Wang, H. Dai, *J. Am. Chem. Soc.* **2001**, *123*, 3838.
[133] H. Jaegfeldt, T. Kuwana, G. Johansson, *J. Am. Chem. Soc.* **1983**, *105*, 1805.
[134] H. Huwe, M. Froba, *Microporous Mesoporous Mater.* **2003**, *60*, 151.
[135] J. J. Lee, S. Han, H. Kim, J. H. Koh, T. Hyeon, S. H. Moon, *Catal. Today* **2003**, *86*, 141.
[136] C. Minchev, H. Huwe, T. Tsoncheva, D. Paneva, M. Dimitrov, I. Mitov, M. Froeba, *Microporous Mesoporous Mater.* **2005**, *81*, 333.
[137] H. Li, S. Zhu, H. a. Xi, R. Wang, *Microporous Mesoporous Mater.* **2006**, *89*, 196.
[138] H. Li, H. a. Xi, S. Zhu, R. Wang, *Mater. Lett.* **2006**, *60*, 943.
[139] H. Huwe, M. Froeba, *Carbon* **2007**, *45*, 304.
[140] Z. Gu, B. Deng, *Environ. Eng. Sci.* **2007**, *24*, 113.
[141] S. Zhu, H. Zhou, M. Hibino, I. Honma, M. Ichihara, *Adv. Funct. Mater.* **2005**, *15*, 381.
[142] S. Zhu, X. Wang, W. Huang, D. Yan, H. Wang, D. Zhang, *J. Mater. Res.* **2006**, *21*, 2847.
[143] K. Wikander, A. B. Hungria, P. A. Midgley, A. E. C. Palmqvist, K. Holmberg, J. M. Thomas, *J. Colloid Interface Sci.* **2007**, *305*, 204.
[144] J. Fan, T. Wang, C. Yu, B. Tu, Z. Jiang, D. Zhao, *Adv. Mater.* **2004**, *16*, 1432.
[145] C. Lin, J. A. Ritter, B. N. Popov, *J. Electrochem. Soc.* **1999**, *146*, 3155.
[146] Y. Zhao, L. Liu, J. Xu, J. Yang, M. Yan, Z. Jiang, *J. Solid State Electrochem.* **2007**, *11*, 449.
[147] J. H. Jang, S. Han, T. Hyeon, S. M. Oh, *J. Power Sources* **2003**, *123*, 79.
[148] S. H. Joo, S. J. Choi, I. Oh, J. Kwak, Z. Lin, O. Terasaki, R. Ryoo, *Nature* **2001**, *412*, 169.
[149] F. Su, J. Zeng, Y. Yu, L. Lu, J. Y. Lee, X. S. Zhao, *Carbon* **2005**, *43*, 2366.
[150] F. Su, J. Zeng, X. Bao, Y. Yu, J. Y. Lee, X. S. Zhao, *Chem. Mater.* **2005**, *17*, 3960.
[151] S. H. Joo, C. Pak, D. J. You, S.-A. Lee, H. I. Lee, J. M. Kim, H. Chang, D. Seung, *Electrochim. Acta* **2006**, *52*, 1618.
[152] J. Zeng, F. Su, J. Y. Lee, X. S. Zhao, J. Chen, X. Jiang, *J. Mater. Sci.* **2007**, *42*, 7191.
[153] J. Zeng, F. Su, J. Y. Lee, W. Zhou, X. S. Zhao, *Carbon* **2006**, *44*, 1713.
[154] F. Su, X. S. Zhao, Y. Wang, J. Zeng, Z. Zhou, J. Y. Lee, *J. Phys. Chem. B* **2005**, *109*, 20200.
[155] M. Schwickardi, S. Olejnik, E.-L. Salabas, W. Schmidt, F. Schueth, *Chem. Commun.* **2006**, 3987.
[156] T. Harada, S. Ikeda, M. Miyazaki, T. Sakata, H. Mori, M. Matsumura, *J. Mol. Catal. A* **2007**, *268*, 59.
[157] A.-H. Lu, W.-C. Li, Z. Hou, F. Schueth, *Chem. Commun.* **2007**, 1038.
[158] A. B. Chen, W. P. Zhang, Y. Liu, X. W. Han, X. H. Bao, *Chin. Chem. Lett.* **2007**, *18*, 1017.
[159] Y. Cao, J. Cao, M. Zheng, J. Liu, G. Ji, H. Ji, *J. Nanosci. Nanotechnol.* **2007**, *7*, 504.
[160] J. M. Cao, Y. L. Cao, X. Chang, M. B. Zheng, J. S. Liu, H. M. Ji, *Stud. Surf. Sci. Catal.* **2005**, *156*, 423.
[161] J.-H. Zhou, J.-P. He, Y.-J. Ji, W.-J. Dang, X.-L. Liu, G.-W. Zhao, C.-X. Zhang, J.-S. Zhao, Q.-B. Fu, H.-P. Hu, *Electrochim. Acta* **2007**, *52*, 4691.
[162] H. Kim, P. Kim, J. B. Joo, W. Kim, I. K. Song, J. Yi, *J. Power Sources* **2006**, *157*, 196.
[163] I.-S. Park, M. Choi, T.-W. Kim, R. Ryoo, *J. Mater. Chem.* **2006**, *16*, 3409.
[164] J. Lee, S. Jin, Y. Hwang, J.-G. Park, H. M. Park, T. Hyeon, *Carbon* **2005**, *43*, 2536.
[165] F. Su, X. S. Zhao, Y. Wang, J. Y. Lee, *Microporous Mesoporous Mater.* **2007**, *98*, 323.
[166] P. Gao, A. Wang, X. Wang, T. Zhang, *Chem. Mater.* **2008**, *20*, 1881.
[167] H. Wang, A. Q. Wang, X. D. Wang, T. Zhang, *Chem. Commun.* **2008**, 2565.
[168] M. Choi, R. Ryoo, *Nat. Mater.* **2003**, *2*, 473.
[169] C. H. Kim, S.-S. Kim, F. Guo, T. P. Hogan, T. J. Pinnavaia, *Adv. Mater.* **2004**, *16*, 736.


© 2008 WILEY-VCH Verlag GmbH & Co. KGaA, Weinheim

[170] Y. S. Choi, S. H. Joo, S.-A. Lee, D. J. You, H. Kim, C. Pak, H. Chang, D. Seung, *Macromolecules* **2006**, *39*, 3275.
[171] Y.-G. Wang, H.-Q. Li, Y.-Y. Xia, *Adv. Mater.* **2006**, *18*, 2619.
[172] H. Talbi, P. E. Just, L. H. Dao, *J. Appl. Electrochem.* **2003**, *33*, 465.
[173] J. W. Long, B. M. Dening, T. M. McEvoy, D. R. Rolison, *J. Non-Cryst. Solids* **2004**, *350*, 97.
[174] N. S. Ergang, J. C. Lytle, K. T. Lee, S. M. Oh, W. H. Smyrl, A. Stein, *Adv. Mater.* **2006**, *18*, 1750.
[175] N. S. Ergang, M. A. Fierke, Z. Wang, W. H. Smyrl, A. Stein, *J. Electrochem. Soc.* **2007**, *154*, A1135.
[176] K. Kageyama, J. Tamazawa, T. Aida, *Science* **1999**, *285*, 2113.
[177] J. L. Figueiredo, M. F. R. Pereira, M. M. A. Freitas, J. J. M. Orfao, *Carbon* **1999**, *37*, 1379.
[178] R. E. Botto, Y. Sanada, in *Advances in Chemistry Series*, Vol. *229*, ACS, Washington DC **1993**.
[179] J. Z. Hu, M. S. Solum, C. M. V. Taylor, R. J. Pugmire, D. M. Grant, *Energy Fuels* **2001**, *15*, 14.
[180] Y. Adachi, M. Nakamizo, *Adv. Chem. Ser* **1993**, *229*, 269.
[181] R. A. Wind, G. E. Maciel, R. E. Botto, *Adv. Chem. Ser.* **1993**, *229*, 3.
[182] X. Zhang, D. H. Solomon, *Chem. Mater.* **1999**, *11*, 384.
[183] C. C. Lin, H. Teng, *Ind. Eng. Chem. Res.* **2002**, *41*, 1986.
[184] Y. Wang, D. Nepal, K. E. Geckeler, *J. Mater. Chem.* **2005**, *15*, 1049.
[185] B. Sakinuna, Y. Yurum, *Microporous Mesoporous Mater.* **2006**, *93*, 304.
[186] G. E. Maciel, C. E. Bronnimann, C. F. Ridenour, *Adv. Chem. Ser.* **1993**, *229*, 27.
[187] H. Knicker, P. G. Hatcher, A. W. Scaroni, *Energy Fuels* **1995**, *9*, 999.
[188] F. Leroux, M. Dubois, *J. Mater. Chem.* **2006**, *16*, 4510.
[189] E. W. Hagaman, S. K. Lee, *Energy Fuels* **1995**, *9*, 727.
[190] P. Painter, M. Starsinic, M. Coleman, *Fourier Transform Infrared Spectrosc.* **1985**, *4*, 169.
[191] C. de Almeida Filho, A. J. G. Zarbin, *Carbon* **2006**, *44*, 2869.
[192] S. Reculusa, B. Agricole, A. Derre, M. Couzi, E. Sellier, P. Delhaes, S. Ravaine, *Electroanalysis* **2007**, *19*, 379.
[193] A. Vinu, P. Srinivasu, M. Takahashi, T. Mori, V. V. Balasubramanian, K. Ariga, *Microporous Mesoporous Mater.* **2007**, *100*, 20.
[194] S. Lei, J. Miyamoto, T. Ohba, H. Kanoh, K. Kaneko, *J. Phys. Chem. C* **2007**, *111*, 2459.
[195] H. Darmstadt, C. Roy, S. Kaliaguine, S. J. Choi, R. Ryoo, *Carbon* **2002**, *40*, 2673.
[196] C. Weidenthaler, A.-H. Lu, W. Schmidt, F. Schueth, *Microporous Mesoporous Mater.* **2006**, *88*, 238.
[197] H. Darmstadt, C. Roy, S. Kaliaguine, S. J. Choi, R. Ryoo, in *Carbon'01. An International Conference on Carbon*, University of Kentucky Center for Applied Energy Research Library, Lexington, Kentucky, **2001**, p. 35.
[198] H. P. Boehm, E. Diehl, W. Heck, R. Sappok, *Angew. Chem.* **1964**, *76*, 742.
[199] S. S. Barton, M. J. B. Evans, E. Halliop, J. A. F. Macdonald, *Carbon* **1997**, *35*, 1361.
[200] D. S. Cameron, S. J. Cooper, I. L. Dodgson, B. Harrison, J. W. Jenkins, *Catal. Today* **1990**, *7*, 113.
[201] M. J. Bleda-Martinez, D. Lozano-Castello, E. Morallon, D. Cazorla-Amoros, A. Linares-Solano, *Carbon* **2006**, *44*, 2642.
[202] M. J. Bleda-Martinez, E. Morallon, D. Cazorla-Amoros, *Electrochim. Acta* **2007**, *52*, 4962.
[203] G. Tremblay, F. J. Vastola, P. L. Walker, Jr, *Carbon* **1978**, *16*, 35.
[204] B. Xiao, J. P. Boudou, K. M. Thomas, *Langmuir* **2005**, *21*, 3400.
[205] F. Rouquerol, J. Rouquerol, K. Sing, *Adsorption by Powders & Porous Solids*, Academic, San Diego, CA **1999**.
[206] S. J. Gregg, K. S. W. Sing, *Adsorption, Surface Area and Porosity*, Academic, London **1982**.
[207] B. Fang, H. Zhou, I. Honma, *J. Phys. Chem. B* **2006**, *110*, 4875.
[208] M. Kruk, M. Jaroniec, A. Sayari, *Langmuir* **1997**, *13*, 6267.
[209] M. Kruk, M. Jaroniec, *J. Phys. Chem. B* **2002**, *106*, 4732.
[210] M. Jaroniec, L. A. Solovyov, *Langmuir* **2006**, *22*, 6757.
[211] J. Choma, J. Gorka, M. Jaroniec, *Microporous Mesoporous Mater.* **2008**, *112*, 573.
[212] P. I. Ravikovitch, A. V. Neimark, *Langmuir* **2002**, *18*, 1550.
[213] M. H. Lim, C. F. Blanford, A. Stein, *Chem. Mater.* **1998**, *10*, 467.
[214] K. Wikander, A. B. Hungria, P. A. Midgley, A. E. C. Palmqvist, K. Holmberg, J. M. Thomas, *J. Colloid Interface Sci.* **2007**, *305*, 204.
[215] D. Lee, J. Lee, J. Kim, J. Kim, H. B. Na, B. Kim, C.-H. Shin, J. H. Kwak, A. Dohnalkova, J. W. Grate, T. Hyeon, H.-S. Kim, *Adv. Mater.* **2005**, *17*, 2828.
[216] C. Z. Lai, M. A. Fierke, A. Stein, P. Bühlmann, *Anal. Chem.* **2007**, *79*, 4621.
[217] C. Z. Lai, M. M. Joyer, M. A. Fierke, N. D. Petkovich, A. Stein, P. Buhlmann, *J. Solid State Electrochem.* **2008**, DOI 10.1007/s10008-008- 0579-2.
[218] T. Wang, X. Liu, D. Zhao, Z. Jiang, *Chem. Phys. Lett.* **2004**, *389*, 327.
[219] W. Xing, Z. F. Yan, G. Q. Lu, R. Ryoo, in *Oz Nano 03. Proceedings of the Asia Pacific Nanotechnology Forum* (Ed.: J. Schulte), World Scientific, Singapore **2004**, p. 45.
[220] H. Zhou, S. Zhu, M. Hibino, I. Honma, M. Ichihara, *Adv. Mater.* **2003**, *15*, 2107.
[221] Y. Wang, F. Su, J. Y. Lee, X. S. Zhao, *Chem. Mater.* **2006**, *18*, 1347.
[222] F. Su, X. S. Zhao, Y. Wang, L. Wang, J. Y. Lee, *J. Mater. Chem.* **2006**, *16*, 4413.
[223] Q. Pan, H. Wang, Y. Jiang, *J. Mater. Chem.* **2007**, *17*, 329.
[224] Q. Pan, H. Wang, Y. Jiang, *Electrochem. Commun.* **2007**, *9*, 754.
[225] C. Lin, J. A. Ritter, B. N. Popov, *J. Electrochem. Soc.* **1999**, *146*, 3639.
[226] J. Lee, S. Yoon, T. Hyeon, S. M. Oh, K. B. Kim, *Chem. Commun.* **1999**, 2177.
[227] T. Hyeon, S. M. Oh, J. Lee, S. Yoon, *Mater. Res. Soc. Symp. Proc.* **2000**, *593*, 193.
[228] S. Yoon, J. Lee, T. Hyeon, S. M. Oh, *J. Electrochem. Soc.* **2000**, *147*, 2507.
[229] W. Li, D. Chen, Z. Li, Y. Shi, Y. Wan, J. Huang, J. Yang, D. Zhao, Z. Jiang, *Electrochem. Commun.* **2007**, *9*, 569.
[230] J. W. Long, D. R. Rolison, *Prepr. Symp. - Am. Chem. Soc, Div. Fuel Chem.* **2006**, *51*, 41.
[231] Q. Meng, L. Liu, H. Song, *J. Appl. Electrochem.* **2006**, *36*, 63.
[232] J. Ding, K.-Y. Chan, J. Ren, F.-S. Xiao, *Electrochim. Acta* **2005**, *50*, 3131.
[233] T. C. Deivaraj, J. Y. Lee, *J. Power Sources* **2005**, *142*, 43.
[234] M.-L. Lin, C.-C. Huang, M.-Y. Lo, C.-Y. Mou, *J. Phys. Chem. C* **2008**, *112*, 867.
[235] H. Du, B. Li, F. Kang, R. Fu, Y. Zeng, *Carbon* **2007**, *45*, 429.
[236] J. Pang, J. E. Hampsey, Z. Wu, Q. Hu, Y. Lu, *Appl. Phys. Lett.* **2004**, *85*, 4887.
[237] R. Gadiou, S.-E. Saadallah, T. Piquero, P. David, J. Parmentier, C. Vix-Guterl, *Microporous Mesoporous Mater.* **2005**, *79*, 121.
[238] Z. Yang, Y. Xia, R. Mokaya, *J. Am. Chem. Soc.* **2007**, *129*, 1673.
[239] A. Pacula, R. Mokaya, *J. Phys. Chem. C* **2008**, *112*, 2764.
[240] T. Roussel, R. J. M. Pellenq, M. Bienfait, C. Vix-Guterl, R. Gadiou, F. Beguin, M. Johnson, *Langmuir* **2006**, *22*, 4614.
[241] L. R. Radovic, F. Rodriguez-Reinoso, *Chem. Phys. Carbon* **1997**, *25*, 243.
[242] E. Auer, A. Freund, J. Pietsch, T. Tacke, *Appl. Catal. A* **1998**, *173*, 259.
[243] K.-I. Min, J.-S. Choi, Y.-M. Chung, W.-S. Ahn, R. Ryoo, P. K. Lim, *Appl. Catal. A* **2008**, *337*, 97.
[244] E. Sipos, G. Fogassy, A. Tungler, P. V. Samant, J. L. Figueiredo, *J. Mol. Catal. A* **2004**, *212*, 245.
[245] M. Hara, T. Yoshida, A. Takagaki, T. Takata, J. N. Kondo, S. Hayashi, K. Domen, *Angew. Chem. Int. Ed.* **2004**, *43*, 2955.
[246] M. Toda, A. Takagaki, M. Okamura, J. N. Kondo, S. Hayashi, K. Domen, M. Hara, *Nature* **2005**, *438*, 178.
[247] J. Lee, D. Lee, E. Oh, J. Kim, Y.-P. Kim, S. Jin, H.-S. Kim, Y. Hwang, J. H. Kwak, J.-G. Park, C.-H. Shin, J. Kim, T. Hyeon, *Angew. Chem. Int. Ed.* **2005**, *44*, 7427.
[248] J. A. Harnisch, D. B. Gazda, J. W. Anderegg, M. D. Porter, *Anal. Chem.* **2001**, *73*, 3954.
[249] A. Vinu, C. Streb, V. Murugesan, M. Hartmann, *J. Phys. Chem. B* **2003**, *107*, 8297.


© 2008 WILEY-VCH Verlag GmbH & Co. KGaA, Weinheim

[250] A. Vinu, M. Miyahara, V. Sivamurugan, T. Mori, K. Ariga, *J. Mater. Chem.* **2005**, *15*, 5122.
[251] M. Hartmann, G. Chandrasekar, A. Vinu, *Chem. Mater.* **2005**, *17*, 829.
[252] A. Vinu, M. Miyahara, T. Mori, K. Ariga, *J. Porous Mater.* **2006**, *13*, 379.
[253] A.-H. Lu, W. Schmidt, N. Matoussevitch, H. Boennemann, B. Spliethoff, B. Tesche, E. Bill, W. Kiefer, F. Schueth, *Angew. Chem. Int. Ed.* **2004**, *43*, 4303.
[254] A.-H. Lu, W.-C. Li, N. Matoussevitch, B. Spliethoff, H. Boennemann, F. Schueth, *Chem. Commun.* **2005**, 98.
[255] H. Yan, C. F. Blanford, J. C. Lytle, C. B. Carter, W. H. Smyrl, A. Stein, *Chem. Mater.* **2001**, *13*, 4314.
[256] M. Kim, K. Sohn, H. B. Na, T. Hyeon, *Nano Lett.* **2002**, *2*, 1383.
[257] A. Stein, *Adv. Mater.* **2003**, *15*, 763.
[258] I. Schmidt, C. Madsen, C. J. H. Jacobsen, *Inorg. Chem.* **2000**, *39*, 2279.
[259] S.-S. Kim, J. Shah, T. J. Pinnavaia, *Chem. Mater.* **2003**, *15*, 1664.
[260] L. Nicole, C. Boissiere, D. Grosso, A. Quach, C. Sanchez, *J. Mater. Chem.* **2005**, *15*, 3598.


© 2008 WILEY-VCH Verlag GmbH & Co. KGaA, Weinheim